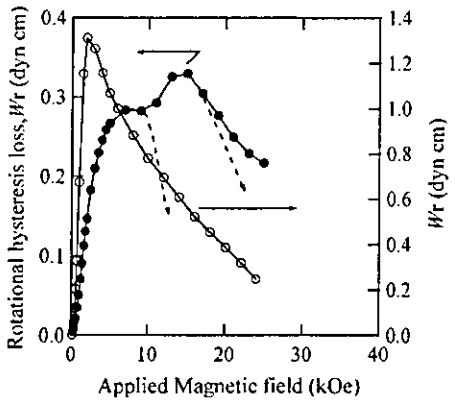

Fig. 5. Rotational hysteresis loss curves for FePt nanoparticles prepared by the modified polyol process measured at RT. Open and closed circles denote the as-synthesized agglomerates and the dispersed nanoparticle monolayered film after annealing at 600 °C, respectively.

for the as-synthesized FePt nanoparticle agglomerates by the modified polyol process is shown. The curve for the 600 °C-annealed film of FePt nanoparticles synthesized by the modified polyol process had two maximum fields (H_p) of about 7 and 15 kOe, leading to two different uniaxial magnetic anisotropy fields (H_k) of at least 14 and 30, respectively, according to classical single domain theory. However, these estimated H_k values were larger than double of the H_c at 5 K with minimal thermal effects. Namely, H_c/H_k of the 600 °C-annealed film indicated smaller value compared to the theoretical one of non-interacting, magnetically isolated Stoner–Wohlfarth-type grains of 0.479 (for random orientation) [20]. We consider this reason to be mainly due to the distribution of H_k of nanoparticles. The magnetization reversal which is characteristic of the polycrystalline particles could not be discussed here because of the existence of this distribution of H_k. Interaction between and within the particles seems not to be dominant in this case because the interparticle coalescence was not likely to occur after annealing and the particles were separated enough. Nevertheless detailed investigation based on some magnetic measurements should be made for further understanding. On the other hand, a single peak was observed for the film composed of as-synthesized nanoparticles by the modified polyol process. It had extremely small H_p value of 200 Oe compared to the estimated H_k of nearly 30 kOe, which is thought to be due to the distribution in the switching field caused by that in the degree of ordering and the exchange coupling between the nanoparticles. The estimated one is considered to be the maximum value in the film.

IV. FePt Nanoparticle Arrays via Template-Assisted Self-Assembly

A. Fabrication Method of Nanoparticle Array

The periodic array of FePt nanoparticles was fabricated using the template-assisted self-assembly technique, which involved scanning probe lithography. The procedure was composed of the following three steps. First, the monolayered octadecyltrichlorosilane (OTS) was formed on a P-type silicon wafer by dipping it in the solution, which allowed the termination of the methyl group on the substrate. Second, the $-CH_3$ terminated

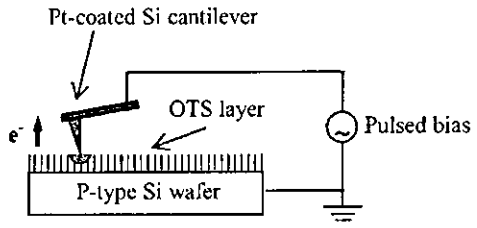

Fig. 6. Schematic diagram for electrochemical patterning of the periodic small dot arays on a $-CH_3$, terminated substrate.

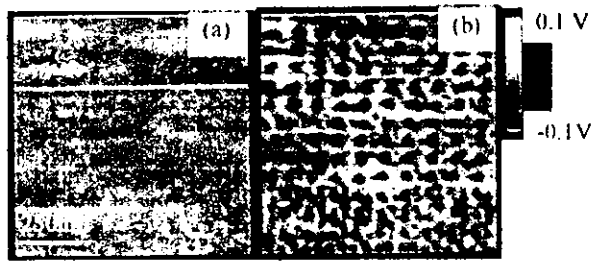

Fig. 7. LFM images of (a) $-CH_3$, terminated (before patterned) and (b) electrochemically patterned surfaces on a Si substrate.

surface was electrochemically modified using a conducting cantilever used in scanning probe microscopes. Fig. 6 shows the schematic diagram for patterning periodic small dot arrays on the substrate. The conducting cantilever was scanned on the substrate with the contact mode, applying a positive pulse bias of 9.5 V with frequency of 20 Hz and 10 ms per pulse. The scanning rate was 2 μm/s. Finally, the modified substrate was immersed in n-hexane based FePt nanoparticle dispersion, then taken out, and rinsed by n-hexane.

The patterned surface was observed using a scanning probe microscope with two different modes, namely, atomic force microscope (AFM) and lateral force microscope (LFM). The observation of the resulting nanoparticle array was carried out using a field emission scanning electron microscope (FE-SEM).

B. Analysis of Patterned Surface and Nanoparticle Array

Fig. 7 indicates LFM images of (a) $-CH_3$ terminated (before patterned) and (b) electrochemically patterned surfaces on a Si substrate. The difference in frictional force is reflected in the contrast as shown in the figure. There was almost no contrast in the image before patterning. Conversely, periodic dark spots, which corresponded to the periodicity of the modification condition, appeared in the image after patterning. Therefore, we recognize these spots as the modified areas. The average diameter of the spots was about 70 nm and they were well aligned with a separation of about 80 nm between centers. Each dark area had relatively higher friction, which meant that $-CH_3$ terminated groups were changed into some polar ones by the electrochemical reaction. Fig. 8 shows the AFM images of (a) $-CH_3$ terminated (before patterned) and (b) electrochemically patterned surfaces. Topographic change after patterning was not observed from the AFM results. Thus, the electrochemical patterning was carried out without any change in roughness of the substrate. The FE-SEM image of the FePt nanoparicle arrays coated on the patterned substrate is shown in Fig. 9. It could be found that FePt nanoparticles were fixed on the patterned areas selectively.

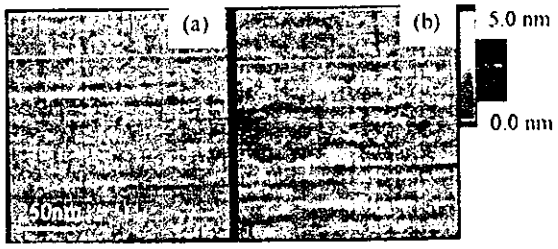

Fig. 8. AFM images of (a) $-CH_3$ terminated (before patterned) and (b) electrochemically patterned surfaces on a Si substrate.

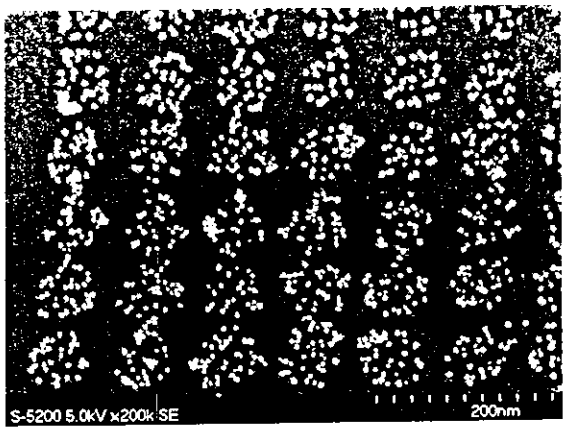

Fig. 9. FE-SEM image of the FePt nanoparticle array coated on the patterned substrate. White dots correspond to the FePt nanoparticles.

The modified polar sites are thought to work as templates for anchoring the nanoparticles effectively. The number of nanoparticles per dot was around 33 with a standard deviation of 4.8 and the dot density corresponded to 0.1 Tparticles/in^2. Ideally, this should be decreased to one particle per dot when the application to recording media is taken into consideration. The possibility of the same is being investigated now. Thus, the template-assisted self-assembly technique to fabricate the periodic nanoparticle array was successfully demonstrated and can be the promising tool for developing future ultrahigh-density recording media.

V. Conclusion

Chemically ordered $L1_0$-type FePt nanoparticles were synthesized directly without surfactants in the solution phase through the co-reduction of Fe(III) and Pt(II) acetylacetonates at 300 °C. These nanoparticles could be dispersed in a nonpolar solvent such as n-hexane by coating the particles with surfactants with long alkyl chains. However, the dispersed particles were of only chemically disordered fcc phase and exhibited superparamagnetic behavior. This may be due to the deficiency of the Fe content caused by the dispersion treatment. An alternative dispersion technique is being developed. The dispersed FePt nanoparticle film stabilized using amino-silane began to structurally transform to the ordered $L1_0$ phase at 600 °C. This phenomenon could be explained by the characteristic polycrystalline nature and the relatively large crystal size of the particles synthesized by the modified polyol process. Rotational hysteresis loss measurement suggested that the nanoparticle film annealed at 600 °C was not completely ordered.

The periodic array of FePt nanoparticles was fabricated using the template-assisted self-assembly technique. For making periodic dots on a substrate, a positive-biased pulse voltage was applied to the $-CH_3$ terminated surface by a conducting cantilever of a scanning probe microscope, which induced electrochemical modification into polar groups. The resulting template had well-aligned sub-100-nm dot arrays with sub-100-nm periodicity. We also succeeded in selectively fixing the FePt nanoparticles on the patterned areas.

References

[1] D. Weller and A. Moser, "Thermal effect limits in ultrahigh-density magnetic recording," *IEEE Trans. Magn.*, vol. 35, no. 6, pp. 4423–4439, Nov. 1999.

[2] S. Sun, C. B. Murray, D. Weller, L. Folks, and A. Moser, "Monodisperse FePt nanoparticles and ferromagnetic FePt nanocrystal superlattices," *Science*, vol. 287, pp. 1989–1992, 2000.

[3] S. Sun, E. E. Fullerton, D. Weller, and C. B. Murray, "Compositionally controlled FePt nanoparticle materials," *IEEE Trans. Magn.*, vol. 37, no. 4, pp. 1239–1243, Jul. 2001.

[4] A. C. C. Yu, M. Mizuno, Y. Sasaki, H. Kondo, and K. Hiraga, "Structural characteristics and magnetic properties of chemically synthesized CoPt nanoparticles," *Appl. Phys. Lett.*, vol. 81, pp. 3768–3770, 2002.

[5] S. Sun, S. Anders, T. Thomson, J. E. E. Baglin, M. F. Toney, H. F. Hamann, C. B. Murray, and B. D. Terris, "Controlled synthesis and assembly of FePt nanoparticles," *J. Phys. Chem. B*, vol. 107, pp. 5419–5425, 2003.

[6] M. Chen and D. E. Nikles, "Synthesis, self-assembly, and magnetic properties of $Fe_xCo_yPt_{100-x-y}$ nanoparticles," *Nano Lett.*, vol. 2, pp. 211–214, 2002.

[7] C. Chen, O. Kitakami, S. Okamoto, and Y. Shimoda, "Large coercivity and granular structure of $CoPt/SiO_2$ films," *IEEE Trans. Magn.*, vol. 35, no. 5, pp. 3466–3468, Sep. 1999.

[8] M. Yu, Y. Liu, A. Moser, D. Weller, and D. J. Sellmyer, "Nanocomposite CoPt:C films for extremely high-density recording," *Appl. Phys. Lett.*, vol. 20, pp. 3992–3994, 1999.

[9] M. Watanabe, M. Masumoto, D. H. Ping, and K. Hono, "Microstrucutre and magnetic properties of FePt-Al-O granular thin films," *Appl. Phys. Lett.*, vol. 76, pp. 3971–3973, 2000.

[10] Z. R. Dai, S. Sun, and Z. L. Wang, "Phase transformation, coalescence, and twinning of monodisperse FePt nanocrystals," *Nano Lett.*, vol. 1, pp. 443–446, 2001.

[11] S. Wang, S. S. Kang, D. E. Nikles, J. W. Harrell, and X. W. Wu, "Magnetic properties of self-organized $L1_0$ FePtAg nanoparticle arrays," *J. Magn. Magn. Mater.*, vol. 266, pp. 49–56, 2003.

[12] B. Jeyadevan, K. Urakawa, A. Hobo, N. Chinnasamy, K. Shinoda, K. Tohji, D. J. Djayaprawira, M. Tsunoda, and M. Takahashi, "Direct synthesis of fct-nanoparticles by chemical route," *Jpn. J. Appl. Phys.*, vol. 42, pp. L350–L352, 2003.

[13] Y. Sasaki, M. Mizuno, A. C. C. Yu, M. Inoue, K. Yazawa, I. Ohta, M. Takahashi, B. Jeyadevan, and K. Tohji, "Crystallographic structures and magnetic properties of $L1_0$-type FePt nanoparticle monolayered films stabilized on functionalized surfaces," *J. Magn. Magn. Mater.*, vol. 282, pp. 122–126, 2004.

[14] C. A. Ross, "Patterned magnetic recording media," *Annu. Rev. Mater. Res.*, vol. 31, pp. 203–235, 2001.

[15] S. Anders, S. Sun, C. B. Murray, C. T. Rettner, M. E. Best, T. Thomson, M. Albrecht, J.-U. Thiele, E. E. Fullerton, and B. D. Terris, "Lithography and self-assembly for nanometer scale magnetism," *Microelectron. Eng.*, vol. 61–62, pp. 569–575, 2002.

[16] A. C. C. Yu, M. Mizuno, Y. Sasaki, M. Inoue, H. Kondo, I. Ohta, D. Djayaprawira, and M. Takahashi, "Fabrication of monodispersive FePt nanoparticle films stabilized on rigid substrates," *Appl. Phys. Lett.*, vol. 82, pp. 4532–4534, 2003.

[17] M. Mizuno, Y. Sasaki, and M. Inoue, "Fabrication of FePt nanoparticle arrays via template-assisted self-assembly," in *Extended Abst. 51th Spr. Meeting Jpn. Soc. Appl. Phys.*, 2004, p. 194.

[18] JCPDS-International Centre for Diffraction Data, 1999.

[19] Y. K. Takahashi, T. Koyama, M. Ohnuma, T. Ohkubo, and K. Hono, "Size dependence of ordering in FePt nanoparticles," *J. Appl. Phys.*, vol. 95, no. 5, pp. 2690–2696, 2004.

[20] E. C. Stoner and E. P. Wohlfarth, "A mechanism of magnetic hysteresis in heterogeneous alloys," *Trans. R. Soc. London*, vol. A240, pp. 599–642, 1948.

JOURNAL OF APPLIED PHYSICS 97, 1 (2005)

Direct synthesis of Pt based $L1_0$ structured nanoparticles (invited)

Migaku Takahashi
New Industry Creation Hatchery Center (NICHe), Tohoku University, Sendai 980-8579, Japan

Tomoyuki Ogawa and Daiji Hasegawa
Graduate School of Engineering, Department of Electronic Engineering, Tohoku University, Sendai 980-8579, Japan

Bafachandran Jeyadevan
Graduate School of Environmental Studies, Ecomaterial Design and Process Engineering, Tohoku University, Sendai 980-8579, Japan

(Presented on 8 November 2004)

Equiatomic FePt and CoPt nanoparticles with the ordered $L1_0$ structure are attractive as ultrahigh density magnetic recording media. In a recent work, chemically synthesized fcc-FePt nanoparticles with narrow size distribution and their self-assembled array with close-packed microstructure has been achieved successfully. However, the particles coalesced during the subsequent annealing step necessary to obtain $L1_0$ FePt nanoparticles. In the present study, we have successfully demonstrated the direct synthesis of $L1_0$ FePt nanoparticles at low temperature of 553 K using the "modified polyol method" without subsequent annealing, whose diameter is 5–10 nm and intrinsic magnetocrystalline anisotropy field (H_k) is 31 kOe. This indicates that precisely controlling the reaction kinetics, especially low reduction rate through optimizing the polyol/Pt mole ratio and type of polyol are very important for directly synthesizing the $L1_0$ FePt nanoparticles. Furthermore, we investigated the size, morphology and composition dependence of the magnetic properties of FePt nanoparticles in order to clarify the $L1_0$ ordering mechanism. As a result, clear evidence of the existence of the critical diameter for the thermodynamical $L1_0$ ordering is not observed in the size range above 2 nm. Furthermore, the recrystallization and sintering process can be a driving force for promoting the $L1_0$ ordering, and hence, Fe and Pt atom diffusion at the grain boundary plays an important role to the $L1_0$ ordering of FePt nanoparticles. © *2005 American Institute of Physics.*
[DOI: 10.1063/1.1851891]

I. INTRODUCTION

Equiatomic FePt and CoPt nanoparticles with the $L1_0$-ordered structure are promising candidates as ultrahigh density magnetic recording media, since the thermal fluctuation of the spins in small nanoparticles would be suppressed by their large magnetocrystalline anisotropy constant (K_u) of the order of 10^7 erg/cm^3.[1] Although chemical synthesis method, so-called "hot-soap methodm," shows high controllability over the formation of particles with narrow size distribution,[2] most of the methods reported so far require an indispensable postannealing step for the transformation from disordered fcc to ordered $L1_0$ phase of FePt or CoPt nanoparticles, which leads to serious coalescence of the same. In addition, the hot-soap method is unsuitable for large-scale production. From the viewpoint of industrial fabrication and physical interest of grain growth, it is important to lower the $L1_0$ phase transition temperature and a method for direct synthesis of ordered $L1_0$ phase (of FePt or CoPt nanoparticles) should be developed as a next key technology. Reasonable success has been achieved by adding a third element (e.g., Cu, Sn, Pb, Sb, Ag, and Bi) that lowers the phase transition temperature through surface segregation.[3,4] However, the reduction of the phase transition temperature using the above methods has been limited and lowering below 673 K still remains a challenge.

In nanoparticles, surface energy that constitutes large part of the total free energy can be a significant factor in structure formation. In addition to thermodynamic effects, reaction kinetics can be strongly size dependent and the free energy barrier height to phase transformation are relatively low in these very small nanoparticles,[5] promoting complex coupled growth-phase transformation behavior. One of the present authors have succeeded various phase formation of Co particles chemically synthesized by a "modified-polyol method."[6–9] The results showed that with the enhancement in reaction kinetics, the particle size was reduced from submicron to few tens of nanometer accompanied with the crystalline structure change from fcc at micron size, coexistence of fcc and hcp in the submicron size and to epsilon and hcp Co at nanometer size. Therefore, reaction kinetics plays an important role for the size reduction of particles and also the phase formation.

While, in the case of synthesis of FePt and CoPt nanoparticles using the "modified polyol method," Fe or Co as well as Pt ions has to be co-reduced. In our previous report for Co particle synthesis, Pt ions not only reduced to Pt metals, but also enhanced and accelerated the reduction of associated metal ions.[6] Similar reduction behavior can be expected in the case of Fe ions (the reduction of Fe alone in polyol is difficult[7]), and could lead to the formation of FePt alloy particles using the polyol method alone rather than a combination of processes used by Sun *et al.*[2]

0021-8979/2005/97(10)/1/0/$22.50

In the present study, we adapted the modified polyol method for the FePt and CoPt nanoparticle synthesis. During the synthesis, the nanoparticles seem to undergo the formation of unstable phases and different crystalline structures are realized for different particle diameters depending on the reaction kinetics. The low reaction rate can be a promising key parameter for realizing low-temperature equilibrium phase of ordered $L1_0$ of FePt or CoPt nanoparticles.

Furthermore, while the $L1_0$ ordering of FePt and CoPt nanoparticles brings about a drastic change in the magnetic properties.[2] Up to now, only the change of coercive force of FePt and CoPt nanoparticle ensemble, was examined.[2,10] However, the observed hysteresis loops of the nanoparticles ensemble includes magnetostatic and exchange interaction between nanoparticles and the intrinsic magnetic property of the particle are not recorded. Therefore, intrinsic magnetic property such as magnetocrystalline anisotropy field $(2K_u/M_s)$ of the nanoparticle itself must be separately clarified from the volume averaged magnetic properties usually represented by hysteresis loop. Namely, both the intrinsic and volume averaged magnetic properties should be widely discussed in connection with structural character such as crystalline structure (poly or single crystalline), size and morphology. The torque magnetometry is very sensitive to evaluate the intrinsic magnetic properties like H_k and their degree of dispersion as already proposed by present authors.[11] In Fig. 1, the rotational hysteresis loss determined by the magnetic torque measurement for CoPt nanoparticles synthesized by polyol method is shown against the applied field, H. Sample A has a unique loss maximum at 1 kOe (defined as H_p) and the hysteresis loss disappears at 31 kOe (defined as H_k) (simple extrapolation). H_p, the field where loss becomes the maximum, shows the volume averaged switching field, which is almost the same as the coercive force of an ensemble of nanoparticles. H_k, the field where the loss vanishes, shows the intrinsic magnetocrystalline anisotropy field of CoPt nanoparticles. The ratio of H_p/H_k is much less than 0.5 suggests the single-phase assembly with clustering and/or multiphase assembly with a large distribution in H_k. On the other hand, sample B has two maxima at 4 kOe and 18 kOe (denoted as H_{p1} and H_{p2}, respectively), and the hysteresis loss disappears at 8 kOe and 31 kOe (denoted as H_{k1} and H_{k2}, respectively). The H_{k2} corresponds with that originating from the CoPt nanoparticles as mentioned above, and the H_{k1} with that from Co nanoparticles. H_{p1}/H_{k1} and H_{p2}/H_{k2} values of 0.5, in this case, suggest that the isolated CoPt with H_{k2} and Co nanoparticles with H_{k1} with three dimensionally random distribution of easy-axis of magnetization coexist. Therefore, the torque magnetometory can be a powerful tool for investigating the intrinsic magnetic properties of nanoparticles and their dispersion state.

Within the framework of the present paper, the atomistic ordering process of FePt nanoparticles in connection with intrinsic magnetic properties, size, morphology, crystalline structure (poly or single crystalline), the change in the degree of ordering, composition, and its dispersion state is precisely investigated as a function of reaction temperature and also the annealing temperature using FePt nanoparticles synthesized by the modified polyol method.

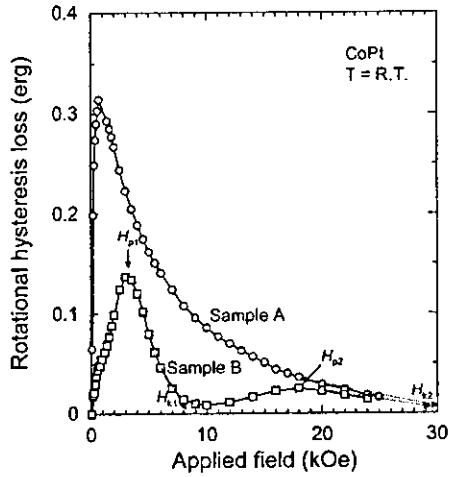

FIG. 1. Rotational hysteresis loss curves at room temperature for CoPt nanoparticles.

II. EXPERIMENTAL PROCEDURE

Specified amounts of Fe acetylacetonate ($Fe(acac)_3$) and Pt acetylacetonate ($Pt(acac)_2$) precursors were dissolved in 100 ml of glycol (ethylene glycol (EG) and tetraethylene glycol (TEG)) in a reaction vessel with a reflux attachment.[12] Then, placed in a mantle heater and heated at a constant rate under gentle mechanical stirring and the suspension was refluxed for three and a half hours at specific temperatures between 473 K and 573 K. During this stage, generally, the pale yellow colored solution turned colorless and finally black suggesting the formation of FePt nanoparticles. The FePt particles thus produced were recovered by centrifuging the suspension and stored in methanol. FePt nanoparticles synthesize at 473 K, which were fixed on a Si substrate using [3-(2-aminoethlyamino)propyl]trimethoxysilane (APTS),[13] were annealed in a vacuum furnace ($\sim 10^{-6}$ Torr) for 30 min in the temperature range from 573 K to 1073 K. The crystalline structure, morphology and composition of as-prepared FePt nanoparticles were analyzed using x-ray diffraction (XRD) with a Cu-K_α line, high-resolution transmission electron microscopy (HRTEM—Hitachi HF2000), TEM-energy disperse x-ray spectroscopy (EDX). The phase transition temperature of as-synthesized FePt nanoparticles was analyzed using differential scanning calorimetry (DSC) in N_2 atmosphere from 323 K to 973 K at a heating rate of 20 K/min. Hysteresis loops were measured using a superconducting quantum interference device (SQUID) magnetometer with maximum applied field of 50 kOe and the rotational hysteresis loss of magnetic torque was measured using a torque magnetometer at room temperature with a maximum applied field of 25 kOe for evaluating the intrinsic magnetic anisotropy field (H_k) of the nanoparticles.

III. RESULTS AND DISCUSSION: STRUCTURE AND MAGNETIC PROPERTIES OF FEPT NANOPARTICLES

A. Reaction temperature dependence

By manipulating the reaction parameters, that is, types of polyol, reaction temperature and metal ion concentration

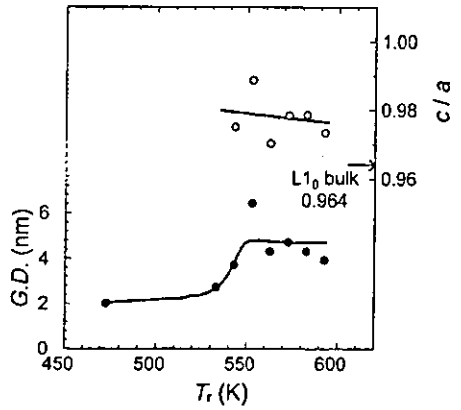

FIG. 2. Reaction temperature dependence of average grain diameter and tetragonality of FePt nanoparticles synthesized by the modified polyol method. The solid lines are guides to the eyes.

(polyol/Pt mole ratio), on the basis of the premises that slow kinetics of the reaction would give ordered FePt nanoparticles. Thus, we tried to synthesize FePt nanoparticles by using ethylene glycol (EG). The as-synthesized FePt nanoparticles having Fe composition ranging between 40 and 60 at %, which was determined by TEM-EDX analysis, were of chemically disordered fcc structure with an average crystallite size of 3–4 nm. The phase transformation temperature, T_t from disordered fcc to ordered $L1_0$ structure determined by DSC measurement was about 573 K under optimum experimental reaction condition. Based on these results, it was found to be difficult to make the $L1_0$ phase successfully because of lower boiling point of EG than T_t. Thus, as a next step, we tried to directly synthesize the $L1_0$ FePt nanoparticles utilizing tetraethylene glycol (TEG) whose boiling point is higher (600 K) than T_t. Furthermore, in the TEG case, the reaction rate can be expected to be slower compared with the EG case. As a result, XRD profiles revealed that the (001) and (110) peaks originating from the $L1_0$ phase were clearly observed above 553 K, indicating that the significant degree of $L1_0$ ordering.

Figure 2 shows the changes of average grain diameter, ⟨G.D.⟩ determined by the Scherrer's equation and tetragonality, c/a of FePt nanoparticles from (200) and (111) peak positions of the XRD data as a function of the reaction temperature, T_r. The ⟨G.D.⟩ value increases from 2 nm at 473 K to ~4 nm in the temperature range of 543–593 K with increasing T_r. The tetragonality, c/a shows around 0.98, which is larger than that of bulk value of 0.964.[14] This suggests the partial $L1_0$ ordering of as-synthesized FePt nanoparticles. Figure 3 shows the TEM images of the FePt nanoparticles in its as-synthesized state as a function of reaction temperature (T_r). From these results, FePt nanoparticles with diameters

FIG. 3. TEM images of FePt nanoparticles synthesized at (a) 533 K, (b) 553 K, and (c) 593 K.

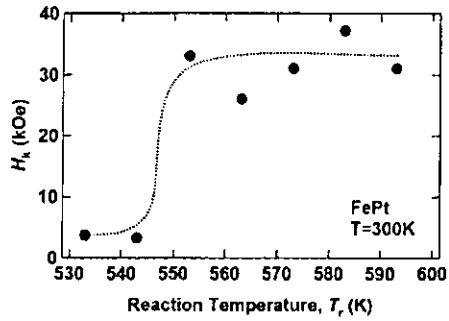

FIG. 4. Reaction temperature dependence of magnetocrystalline anisotropy field of FePt nanoparticles. The dotted lines are guides to the eyes.

ranging between 5–10 nm were observed, which were seriously coalesced with each other. This coalescing behavior always appear in the reaction temperature range between 533 K and 573 K.

Figure 4 shows the reaction temperature dependence of the intrinsic magnetocrystalline anisotropy field (H_k) of the as-synthesized FePt nanoparticles evaluated from torque loss analysis. From this result, H_k shows an abrupt increase from 3.5 kOe to 31 kOe at around 550 K. The high H_k value indicates the $L1_0$ phase formation of FePt nanoparticles above 550 K. The value of c/a in Fig. 2 does not reach to the bulk value of $L1_0$ phase above 550 K. Thus, the values of H_k ~3.5 kOe and ~31 kOe can be explained in terms of partial $L1_0$ ordering of FePt nanoparticles. The values of H_p/H_k are much less than 0.5 due to a strong exchange coupling between the FePt nanoparticles in the reaction temperature range from 553 K to 593 K, suggesting the serious coalescence of FePt nanoparticles as supported by the TEM observation in Fig. 3. In order to make further discussion of the $L1_0$ ordering mechanism much clearer, in the next section, size, morphology, and crystalline structure of well-dispersed FePt nanoparticles are precisely investigated as a function of annealing temperature in connection with the magnetic properties.

B. Annealing temperature dependence

Figures 5(a) and 5(b) show TEM images of FePt nanoparticles synthesized at 473 K by modified polyol method and those synthesized at 560 K by conventional hot-soap method, respectively. From Fig. 5(a), well-dispersed polycrystalline FePt nanoparticles with the average diameter of ~7 nm were observed, that is, each FePt nanoparticle contains three to five subgrains of 2–3 nm. From Fig. 5(b), on the other hand, single-crystalline FePt nanoparticles with the average diameter of ~4 nm were observed. The polycrystalline structure of the FePt nanoparticles synthesized by the "modified polyol method" is found to be clearly different from the single-crystalline structure of those by the hot-soap method. This significant difference in the morphology of the nanoparticles can be explained in terms of the difference of the reaction condition between modified polyol method and hot-soap one. Especially, the absence of surfactant during the synthesis of FePt using the modified polyol process is considered to be the reason for the formation of the agglomerates consisting of three-to-five subgrains. This was confirmed

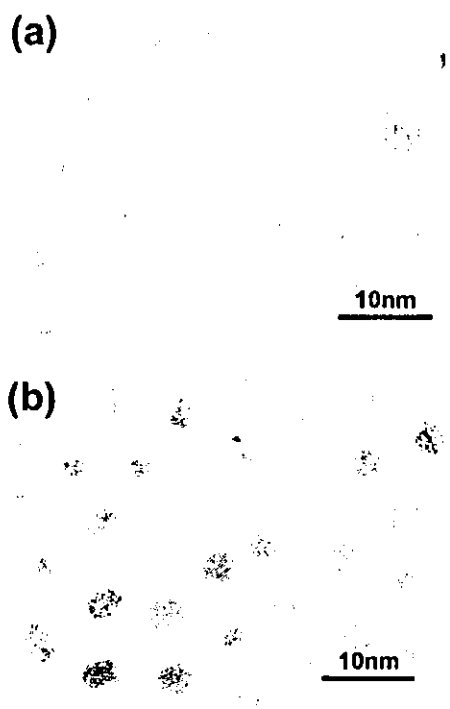

FIG. 5. TEM images of FePt nanoparticles synthesized by (a) modified polyol method and (b) hot-soap method.

by synthesizing FePt nanoparticles in the presence of varying amounts of oleic acid. The degree of agglomeration was a function of surfactant concentration and could be avoided by using appropriate amount.

Figure 6 shows the changes of average grain diameter, ⟨G.D.⟩ determined by the Scherrer's equation, tetragonality, c/a of FePt nanoparticles from (200) and (111) peak positions of the XRD data and order parameter S [relative intensity of $I_{(110)}/I_{(111)}$] by annealing. The ⟨G.D.⟩ value monotonically increases from 2 nm at 573 K to 12 nm at 1073 K with increasing annealing temperature, T_a. The ⟨G.D.⟩ value of 2 nm for as-synthesized FePt nanoparticles is roughly same as the subgrain size obtained from the TEM observation in Fig. 5(a). The ⟨G.D.⟩ value at 873 K is almost same as the average particle diameter of 7 nm obtained from the TEM observation. Our recent study on a self-assembled array of FePt nanoparticles fixed on the APTS layer revealed that the coalescence between nanoparticles was minimal during the annealing process and that the APTS acts as a antisintering material even at 873 K.[13] Therefore, the increment of ⟨G.D.⟩ against T_a can be interpreted in terms of two kinds of grain growth mechanisms dependent on annealing temperature range. One is intraparticle recrystallization seen below 873 K through the atom diffusion process at grain boundary within each nanoparticle and the other interparticle sintering above 873 K due to coalescence of the nanoparticles with each other. On the other hand, the tetragonality, c/a gradually decreases from 0.99 at 573 K and above 773 K monotonically to 0.96 with increasing T_a. The value of c/a at 573 K is smaller than that of disordered fcc phase (1.00) and c/a at 1073 K is almost same as that of $L1_0$ bulk value of 0.964.[14] This indicates the partial $L1_0$ ordering starts even at 573 K and is gradually promoted with increasing T_a. The order parameter, S shows an abrupt increase from 0 at 773 K to 0.83 at 873 K and increases to 0.92 at 1073 K. Below 773 K, the (110) peak originating from the $L1_0$ phase is undetectable due to the small size of the particle. On the contrary, in the hot-soap case, the size of the nanoparticles determined by TEM and ⟨G.D.⟩ by XRD is the same (4 nm), and furthermore the particle morphology is single crystalline. ⟨G.D.⟩ of 4 nm at 873 K increases to 7 nm at 1073 K due to interparticle sintering. In accordance with this increment of ⟨G.D.⟩, c/a relatively reduces from 1 to 0.954. These results suggest that for the FePt nanoparticles synthesized by modified polyol and hot-soap methods, chemically atomistic ordering from fcc to $L1_0$ has a strong correlation with the particle size. The detailed mechanism will be discussed in the next section in connection with the change of magnetic properties as mentioned in the following paragraph.

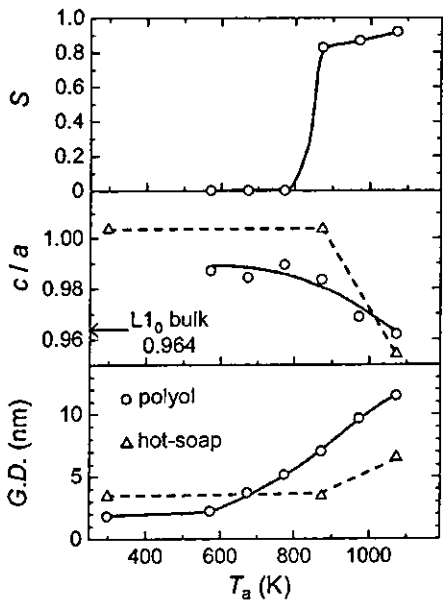

FIG. 6. Annealing temperature dependence of average grain diameter, tetragonality, and order parameter of FePt nanoparticles synthesized by the modified polyol method (circle symbols) and hot-soap method (triangle symbols).

In Fig. 7, the values of H_k and H_p/H_k at 300 K evaluated from the rotational hysteresis loss analysis of torque magnetometry and the saturation field (denoted as H_{sat}) at 5 K from the magnetization curve are shown as a function of T_a. As T_a increases, the abrupt increase in H_k is observed from 0 (<773 K) to 40 kOe (773 K–1073 K). On the other hand, H_{sat} measured at 5 K gradually increases from 15 kOe with increasing T_a and shows a saturation value of 40 kOe. This suggests the partial $L1_0$ ordering of the FePt nanoparticles even in the low temperature range of 573 K–773 K, which corresponds with the result of c/a as shown in Fig. 6. Based on the Arrhenius–Néel model, assuming that the magnetization of FePt nanoparticles at T_a=1073 K is the same as that for the bulk value, the value of $K_u V/k_B T<4.8$ can be obtained for the FePt nanoparticles annealed in the temperature range of 573 K–673 K. In order to observe the ferromag-

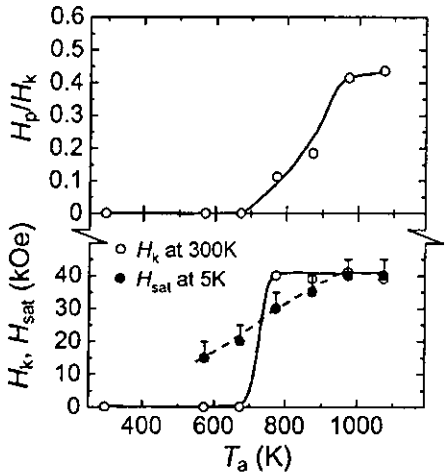

FIG. 7. Annealing temperature dependence of H_k, H_p/H_k at 300 K (open symbols) and H_{sat} at 5 K (solid symbols) of FePt nanoparticles.

netic behavior of magnetic nanoparticles, on the other hand, the relaxation time for the magnetization reversal should be much longer than the observation time scale of magnetic measurement (~100 s), which means $K_uV/k_BT>25$. The smaller value of $K_uV/k_BT<4.8$ indicates the superparamagnetism at 300 K. Therefore, the observed abrupt change in H_k at T_a=773 K can be interpreted as the superparamagnetic contribution originating from partial $L1_0$ ordering of FePt nanoparticles, which suppresses the gradual change of H_k.

H_k of 40 kOe is much smaller than the bulk value of 116 kOe. The smaller value of H_k can be explained in terms of chemical composition fluctuation of FePt nanoparticles. From TEM-EDX analysis in Table I,[15] high composition fluctuation of FePt nanoparticles synthesized by the hot-soap method appears in the local area containing the number of analyzed particle less than 10, whereas the averaged chemical composition is almost the same as the stoichiometry from x-ray microprobe analysis (XMA) within the wide area containing more than 10^6 particles. As a consequence, Pt-rich and Fe-rich FePt nanoparticles shows the small H_k.[16]

H_p/H_k shows a gradual change from 0 to 0.2 with increasing T_a from 573 to 873 K and reaches to saturated value of 0.45 above 973 K. This value is almost same as that (0.479) for the ideal coherent rotation of magnetizations with 3D random distribution of easy-axis of magnetization in each FePt nanoparticle.[17] A smaller value of H_p/H_k less than 0.5 is the consequence of the contributions of a large switching field distribution due to either an exchange coupling between

TABLE I. Chemical composition of FePt naonparticles synthesized by the hot-soap method.

	The number of analyzed particles	Fe (at %)	Pt (at %)
XMA	$\geqslant 10^6$	48	52
TEM-EDX	<10	47.7	52.3
		44.3	55.7
		43.8	56.2
		38.8	61.2
		30.6	69.4

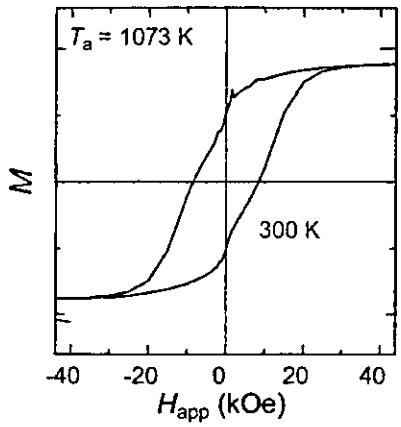

FIG. 8. Hysteresis loop at 300 K of FePt nanoparticles after annealing at 1073 K.

subgrains in each FePt nanoparticle and/or partial $L1_0$ ordering in each FePt nanoparticle emsemble.

In Fig. 8, the hysteresis loop at 300 K of FePt nanoparticles after annealing at 1073 K is shown. For the case of ideal coherent rotation of magnetizations with 3D random distribution of easy-axis of magnetization, H_c/H_k is expected to be about 0.48. However, the coercive force observed experimentally is 8 kOe in spite of H_p/H_k~0.5, which is completely smaller than the expected value of about 20 kOe. This huge discrepancy arises from the large chemical composition fluctuation of FePt nanoparticles as shown in Table I. The existence of a relatively soft-magnetic phase observed in the magnetization behavior at low field range ~1 kOe is reasonably understood by the chemical composition fluctuation. Furthermore, from our recent analysis of residual magnetization, we could separately evaluate the switched component of magnetization from the rotational one and obtain residual coercivity, H_{cr}, of 13 kOe, which was larger than H_c and still lower than that expected from H_p/H_k~0.5. Thus, the lower H_c value of 8 kOe can be explained in terms of not only large chemical composition fluctuation but also rotational mode of magnetization reversal process, which may be due to magnetostatic interaction between FePt nanoparticles. Therefore, to obtain much higher H_k and H_c of FePt nanoparticles, more precise control of chemical composition in each nanoparticle is indispensable in future work.

C. $L1_0$ ordering mechanism of FePt nanoparticles

We will here discuss the $L1_0$ ordering mechanism of FePt nanoparticles. From Figs. 6 and 7, as T_a increases, the ⟨G.D.⟩ value monotonically increases and c/a begins to decrease at 573 K towards the bulk value of the $L1_0$ phase, which corresponds with the increase in H_{sat} as mentioned in the previous section. This may suggest some correlation between ⟨G.D.⟩ and $L1_0$ ordering, namely size dependent ordering process. In Fig. 9, H_{sat}, c/a and S are plotted against ⟨G.D.⟩. A recent experimental work on FePt granular films has proposed[18] that some critical diameter around ~5 nm exists for the thermodynamical $L1_0$ ordering of FePt particles as also plotted in the result of c/a, below which the $L1_0$ ordering cannot take place. The coercive force, in addition, was not observed at 300 K below 4 nm, which was

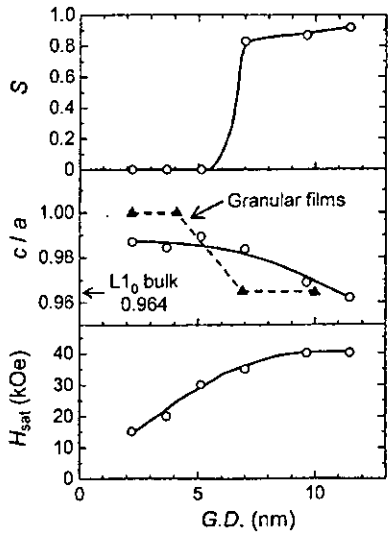

FIG. 9. ⟨G.D.⟩ dependence of H_{sat}, c/a, and S. The triangle symbols show the results of FePt granular film reported in Ref. 17.

interpreted as superparamagnetic behavior of disordered fcc FePt nanoparticles. Thus the partial $L1_0$ ordering of the FePt nanoparticles could not be identified in the small size range below 4 nm. On the other hand, in the present experiment in Fig. 9, the gradual increase in H_{sat} at 5 K and decrease in c/a are found even in the small size range of 2–5 nm. This result suggests that the $L1_0$ ordering is gradually promoted with increasing ⟨G.D.⟩ and the evidence for the existence of the critical diameter for the thermodynamical $L1_0$ ordering is not observed in the size range above 2 nm. That means, the gradual change of H_{sat} may be due to insufficient annealing time for completing the second order phase transition from fcc to $L1_0$ phase accompanied with atom diffusion process of Fe and Pt atoms and/or intrinsic partial $L1_0$ ordering of FePt nanoparticles. The latter partial ordering mechanism in the FePt nanoparticles will be supported by a recent Monte Carlo simulation study of thermodynamic phase transition of the FePt nanoparticle, where the $L1_0$ ordering partially occurs in the FePt nanoparticle with the diameter of 3.5 nm.[19]

We will focus on the correlation between particle morphology and ordering mechanism. From Fig. 6, the ⟨G.D.⟩ increases monotonically via the recrystallization of subgrains in each FePt nanoparticle in the low annealing temperature range and sintering of the FePt nanoparticles in the high annealing temperature range. On the other hand, in the case of FePt nanoparticles synthesized by the hot-soap method, as T_a increases, ⟨G.D.⟩ and c/a remained unchanged even after annealing at 873 K as is shown in Fig. 6, and then at 1073 K, the ⟨G.D.⟩ became larger (7 nm) due to interparticle sintering and c/a reached the bulk value of the $L1_0$ phase. Thus, the recrystallization of subgrains in each FePt nanoparticles and sintering of FePt nanoparticles strongly correlates with the $L1_0$ ordering of FePt nanoparticles. The $L1_0$ ordering occurred by a phase transition over the free energy barrier height by thermal activation from nonequilibrium fcc phase to thermal equilibrium $L1_0$. The barrier height strongly depends on the atomic scale structure such as grain boundary, vacancy, and impurity, which brings about reduction of the height compared to that for a perfect single crystalline structure. Thus, the recrystallization and sintering process can be a driving force for promoting the $L1_0$ ordering and hence, Fe and Pt atom diffusion at the grain boundary plays an important role to the $L1_0$ ordering of FePt nanoparticles.

IV. CONCLUSION

We have successfully demonstrated the direct synthesis of $L1_0$ FePt nanoparticles at a low temperature of 553 K using the "modified polyol method" without subsequent annealing procedure, whose diameter and intrinsic magnetocrystalline anisotropy field (H_k) are 5–10 nm and 31 kOe, respectively. We also found that the reaction kinetics parameters such as polyol/Pt salt mole ratio and type of polyol are very important for directly synthesizing the $L1_0$ FePt nanoparticles. We investigated the size, morphology, and composition dependence of the magnetic properties of FePt nanoparticles in order to clarify the $L1_0$ ordering mechanism. Clear evidence of the existence of the critical diameter for the thermodynamical $L1_0$ ordering is not obtained in the size range above 2 nm. Furthermore, the recrystallization and sintering process can be a driving force for promoting the $L1_0$ ordering, and hence, Fe and Pt atom diffusion at the grain boundary plays an important role to the $L1_0$ ordering of FePt nanoparticles.

ACKNOWLEDGMENTS

This work was supported in part by the IT-program (RR2002) of MEXT and Grant-in-Aid for Basic Research #(B) 15360003 from the Ministry of Education, Science, Culture, and Sport of Japan.

[1]D. Weller and A. Moser, IEEE Trans. Magn. **35**, 4423 (1999).
[2]S. Sun, C. B. Murray, D. Weller, L. Folks, and A. Moser, Science **287**, 1989 (2000).
[3]O. Kitakami, Y. Shimada, K. Oikawa, H. Daimon, and F. Fukamichi, Appl. Phys. Lett. **78**, 1104 (2001).
[4]S. Kang, J. W. Harrell, and D. E. Nikles, Nano Lett. **2**, 1033 (2002).
[5]A. A. Gribbs and J. F. Banfield, Am. Mineral. **82**, 717 (1997).
[6]B. Jeyadevan, O. P. Perez, C. N. Chinnasamy, K. Shinoda, K. Tohji, and A. Kasuya, Dig. 26th Annual Conf. Magnetics in Japan 2002, Tokyo, p. 36.
[7]G. Viau, F. Fievet-Vincent, and F. Fievert, J. Mater. Chem. **6**, 1047 (1996).
[8]O. Perales-Perez, B. Jeyadevan, N. Chinnasamy, K. Tohji, and A. Kasuya, Proc. Int. Symp. Cluster Assembled Materials, Nagoya, 2001 (IPAP, Tokyo, 2001) IPAP Conf. Ser. 3, 105.
[9]B. Jeyadevan, O. P. Perez, C. N. Chinnasamy, K. Shinoda, and K. Tohji, MMMIJ Meet., 133 (2002).
[10]B. Rellinghaus, S. Stappert, M. Acet, and E. F. Wassermann, J. Magn. Magn. Mater. **266**, 142 (2003).
[11]M. Takahashi and T. Shimatsu, IEEE Trans. Magn. **28**, 3285 (1992).
[12]B. Jeyadevan, K. Urakawa, A. Hobo, N. Chinnasamy, K. Shinoda, K. Tohji, D. D. J. Djayaprawira, M. Tsunoda, and M. Takahashi, Jpn. J. Appl. Phys., Part 1 **42**, L350 (2003).
[13]A. C. C. Yu, M. Mizuno, Y. Sasaki, M. Inoue, H. Kondo, I. Ohta, D. Djayaprawira, and M. Takahashi, Appl. Phys. Lett. **82**, 4352 (2003).
[14]JCPDS-International Centre for Diffraction Data 1999.
[15]Y. Sasaki, M. Mizuno, A. C. C. Yu, M. Inoue, K. Yazawa, I. Ohta, M. Takahashi, B. Jeyadevan, and K. Tohji, J. Magn. Magn. Mater. (in press).
[16]K. Barmak, J. Kim, L. H. Lewis, K. R. Coffey, M. F. Toney, A. J. Kellock, and J. U. Thiele, J. Appl. Phys. **95**, 7501 (2004).
[17]E. C. Stoner and E. P. Wohlfarth, Philos. Trans. R. Soc. London, Ser. A **240**, 599 (1948).
[18]Y. K. Takahashi, T. Ohkubo, M. Ohnuma, and K. Hono, J. Appl. Phys. **93**, 7166 (2003).
[19]R. V. Chepulskii, J. Velev, W. H. Butler, M. Takahashi, T. Ogawa, and D. Hasegawa (private communication).

JOURNAL OF APPLIED PHYSICS 97, 1 (2005)

Structural and magnetic properties of monolayer film of CoPt nanoparticles synthesized by polyol process

M. Mizuno, Y. Sasaki, and M. Inoue
Sony Corporation, Sendai Technology Center, Tagajo, Miyagi 985-0842, Japan

C. N. Chinnasamy, B. Jeyadevan,[a] D. Hasegawa, T. Ogawa, M. Takahashi, and K. Tohji
Tohoku University, Aoba-ku, Sendai 980-8579, Japan

K. Sato and S. Hisano
Dowa Mining Co. Ltd., 1-3-1 Kaigandori, Okayama 702-8506, Japan

(Presented on 11 November 2004)

$Co_{43}Pt_{57}$ nanoparticle dispersion was synthesized by using the polyol process, and monolayer film of the particles with [3-(2-aminoethylamino)propyl]trimethoxysilane coupling layer on a silicon substrate was fabricated and characterized. After the film was annealed at 873 K, the $Co_{43}Pt_{57}$ nanoparticles transformed from their as-deposited fcc phase to $L1_0$ structure. However, the resulting c/a ratio was only 0.993, indicating incomplete transformation. Grain size of the annealed film was 4.9 nm against 4.1 nm for the as-deposited state. The annealed film showed the presence of high anisotropic phase with the remanence coercivity of 4.2 kOe and anisotropy field over 25 kOe at RT. © *2005 American Institute of Physics*. [DOI: 10.1063/1.1845811]

I. INTRODUCTION

In the year 2000, chemical synthesis of fcc FePt nanoparticles and their use as the basic unit for recording media were demonstrated.[1] Most of the effort was concentrated on either formulating the techniques to lower the phase transformation temperature (from fcc to $L1_0$ phase)[2–4] or the direct synthesis of $L1_0$ phase.[5,6] We have previously reported the direct synthesis of $L1_0$ FePt nanoparticles by using the polyol process. However, further processing was very difficult because the obtained particles were not dispersible in any solvent, since the particles were agglomerated due to the polymerization of the polyol during the synthesis. only a few reports on the syntheses of CoPt nanoparticles have been described, and, in most cases, the as-synthesized CoPt nanoparticles hve been know to exhibit supermagnetism[7,8] at room temperature. Recently, a similar polyol method has been applied to the synthesis of as-synthesized ferromagnetic CoPt nanoparticles.[9] In this case, to our surprise, the polyol does not undergo polymerization during the synthesis, and does not hinder dispersion. In this article, we report the structural and magnetic properties of monolayer film of the CoPt nanoparticles.

II. EXPERIMENT

A. Synthesis of CoPt nanoparticles

Tetraethylene glycol (TEG, b.p. ~597 K) was used both as solvent and reducing agent. Cobalt (II) acetylacetonate (0.01 M) and platinum (II) acetylacetonate (0.01 M) were used as the cobalt and platinum sources, respectively. The solution was heated to 563 K and refluxed for about 3 h and 30 min, respectively. The black solution was subsequently cooled down to room temperature, centrifuged, and washed with ethanol to collect the CoPt nanoparticles.

B. Fabrication of CoPt nanoparticles monolayer film

The CoPt nanoparticle monolayered film was fabricated as follows: an oxidized silicon wafer was immersed into a toluene solution of [3-(2-aminoethylamino)propyl]trimethoxysilane (APTS) [0.10% (v/v)] for 10 min and then rinsed with toluene, dried, and baked at 120 °C in an oven for 30 min; subsequently, the APTS-derivative substrate was treated with a hexane dispersion of the CoPt nanoparticles (1 mg/mL) for 10 min, followed by rinsing with hexane and dried, yielding a APTS/(CoPt nanoparticle monolayer) bilayer heterostructure.[10] The as-deposited film was then annealed under a vacuum of 10^{-7} Torr at temperatures from 673 to 1173 K at 100-degree intervals to evaluate the crystallographic features and magnetic properties.

C. Characterization

The structure, morphology, composition, and magnetic properties of the as-prepared CoPt particles were analyzed using x-ray diffraction (XRD) (Rigaku—Cu-K_α radiation), high-resolution transmission electron microscopy (HR-TEM, Hitachi HF2000), TEM-energy dispersive x-ray spectroscopy (EDX), and vibrating sample magnetometer (VSM), respectively. The observation of the particles in the monolayered film was carried out using a field emission scanning electron microscope (FE-SEM, Hitachi S-5200). The anisotropy field (H_k) was measured by using a torque magnetometer (Tamagawa) at room temperature with a maximum applied field up to 25 kOe. In order to investigate the phase transformation temperature (T_t), differential scanning calorimetric (DSC, Rigaku DSC-8270) studies were performed in N_2 atmosphere. The crystallographic textures and average grain sizes of the CoPt monolayered films were evaluated by in-plane

[a]Electronic mail: jeya@mail.kankyo.tohoku.ac.jp

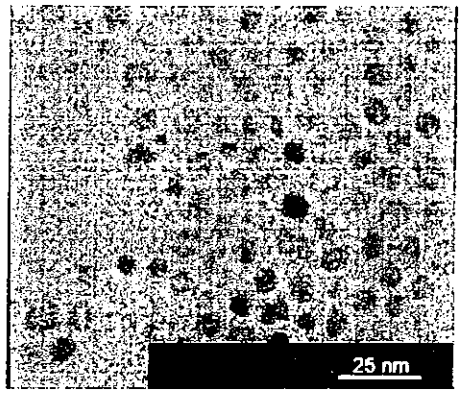

FIG. 1. TEM micrograph of $Co_{43}Pt_{57}$ nanoparticles.

x-ray diffraction(XRD) measurements with the x-ray incident angle set at 0.25 deg. from the plane (Rigaku ATX-G with Cu K_α radiation).

III. RESULTS AND DISCUSSION

A. Preparation of CoPt nanoparticles dispersion

The size and composition of CoPt nanoparticles were tuned by controlling the heating rate and other experimental conditions. The average composition was found to be $Co_{43}Pt_{57}$ by TEM-EDX analysis. The saturation magnetization (M_s) and the coercivity (H_c) of the powder were 29 emu/g and 50 Oe, respectively. The large value of M_s may be due to the presence of a minor fraction of partially ordered CoPt nanoparticles in the as-prepared state itself. In other words, the as-prepared CoPt nanoparticles have enough anisotropy to be ferromagnetic at room temperature. Rotational hysteresis loss (W_r) for the as-prepared CoPt nanoparticles plotted as a function of applied magnetic field up to 25 kOe, showed an H_k of about 21.4 kOe and confirmed the presence of CoPt particles with fractionally ordered structure. DSC studies showed that the T_t was about 570 K ($peak_{onset}$ temperature). Compared with the bulk CoPt alloy, T_t was reduced by about 525 K without doping any third elements. Thus, to analyze the potential of these particles, the as-prepared ferromagnetic CoPt particles were dispersed in an organic solvent using either oleylamine and/or oleic acid as surfactants. The appropriate amounts of surfactants were introduced into the CoPt–polyol suspension. Subsequently, the suspension was agitated for 10 h using a mechanical shaker. Then, a nonpolar solvent such as hexane was added to the suspension and agitated further. During this process, the particles got coated with the surfactants and were transferred from the polyol medium to hexane. The TEM micrograph of the dispersed particles is shown in Fig. 1. The particles were nearly spherical in shape and the average particle size was about 7 nm with ±2.5 nm size distribution.

B. CoPt nanoparticles monolayer film

The in-plane XRD for the as-deposited and 873 K annealed CoPt nanoparticles monolayered films are shown in Fig. 2. Furthermore, the observation of chemically ordered $L1_0$ (110) superlattice reflection was realized for the sample

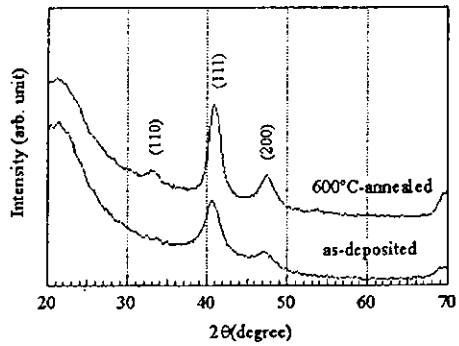

FIG. 2. In-plane XRD of the as-deposited and 873 K annealed $Co_{43}Pt_{57}$ particles.

annealed at 873 K in vacuum. The c/a ratio, calculated using the (111) and (200) peaks, was 0.9926 as compared to the value of 0.9732 observed for complete ordering. Note that unlike in the case of FePt particles synthesized by the IBM method where the super lattice peaks began to appear only at temperatures as high as 1073 K.[10,11] The FE-SEM of the monolayer film annealed at 873 K is shown in Fig. 3. The grain diameters of the nanoparticles film were calculated using the Scherrer's equation using the full-width at half-maximum (FWHM) of the (111) peak. This suggested that the growth of the particles through coalescence has been restricted and the average diameter was 4.9 nm as compased to 4.1 nm for the as-deposited case. This increase may be due either to the slight sintering of the particles in the film or to the transformation of the polycrystals, which is the case for the particles synthesized in tetraethylene glycol, to single crystal.

C. Magnetic properties of CoPt nanoparticle monolayer film

The in-plane hysteresis loops of the as-deposited CoPt nanoparticle monolayer film at room temperature and 5 K are shown in Fig. 4. The film showed a coercivity of about 20 Oe (slightly different from the data of the powder) at RT; however, the coercivity at 5 K was about 730 Oe. This suggested that the particles are superparamagnetic at RT and was consistent with the fcc structure. The hysteresis loops of the 873 K annealed film measured at RT and 5 K are shown in Fig. 5. The 873 K annealed film showed a coercivity of

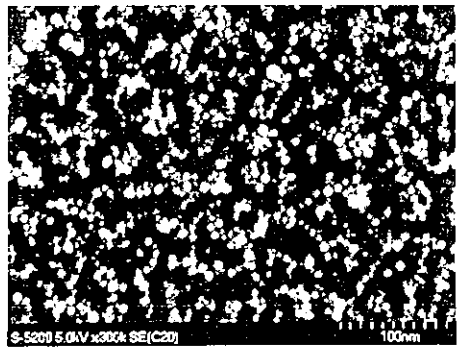

FIG. 3. FE-SEM of the monolayer $Co_{43}Pt_{57}$ film annealed at 873 K.

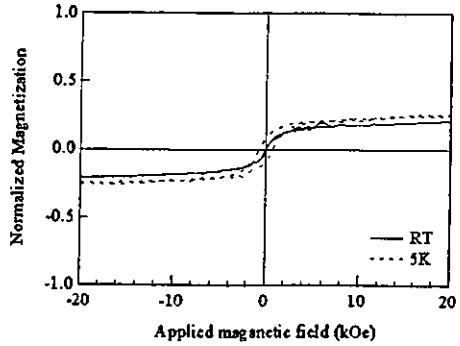

FIG. 4. In-plane hysteresis loop of the (a) as-deposited $Co_{43}Pt_{57}$ monolayer film measured at 300 and 5 K (magnetization is normalized by that of the 873 K-annealed film measured at 5 K under 50 kOe).

about 160 and 1900 Oe at RT and 5 K, respectively. This suggested that most of the particles are superparamagnetic at RT. However, this was inconsistent with the crystallographic data, which suggested the presence of a high, anisotropic ordered phase. Thus, to investigate the presence of $L1_0$ phase in the CoPt particle film annealed at 873 K, in-plane measurements of the remanence coercivity (H_{cr}) and the intrinsic magnitude of the magnetic anisotropy field, H_k, were measured. The DCD curve measured with a saturation field of 50 kOe recorded an H_{cr} value of about 4200 Oe at RT (Fig. 5). This suggested the presence of at least two phases with low and high anisotropies in the film. The H_k value was evaluated to be above 25 kOe and confirmed the presence of highly anisotropic phase as shown in Fig. 6. The reason for the existence of the low anisotropy phase can be due to the distribution of ordering. This can be due to the variation in composition between particles and/or particle size. Though the overall composition of the particles was $Co_{43}Pt_{57}$, we could observe particles rich in cobalt. Note that the fraction of such particles was small. The other possible reason is the dependence of phase stability on particle size. Recently, it was claimed that the fcc structure is stable when the particle diameter of FePt is less than 4 nm in $FePt/Al_2O_3$ and $FePt/SiO_2$ granular films.[12] Hence, it is believed that the

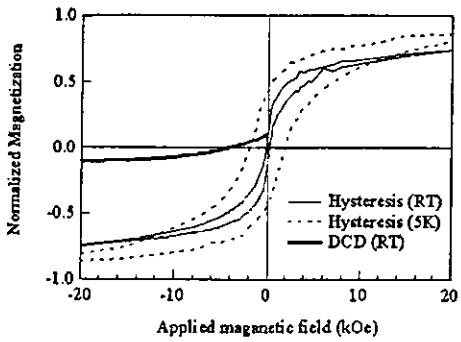

FIG. 5. In-plane hysteresis loop and DCD curve of the 873 K-annealed $Co_{43}Pt_{57}$ monolayer film measured at 300 and 5 K.

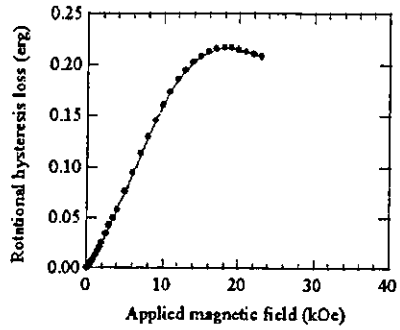

FIG. 6. Rotational hysteresis loss curve of the 873 K-annealed $Co_{43}Pt_{57}$ monolayer film measured at RT.

synthesis of CoPt with average diameters greater than 7 nm with narrow size distribution could be a potential candidate as these particles synthesized through polyol process are easily dispersible compared to FePt nanoparticles synthesized by similar route.

IV. CONCLUSIONS

Ferromagnetic 7 nm CoPt nanoparticles were prepared by using the modified polyol process. The monolayer film of CoPt nanoparticles was fabricated by the application of APTS as a coupling layer. The grain growth was well controlled even after annealing at higher temperatures. The presence of the highly anisotropic $L1_0$ nm phase was confirmed by x-ray and rotational hysteresis loss analyses.

ACKNOWLEDGMENTS

This study was supported by Grant-in-Aid for Basic Research No. (B)15360003, No. (S)14103016, and No. (S)13852016 from the Ministry of Education, Science, Culture and Sport of Japan and No. H14-nano-021 from the Ministry of Health, Labor and Welfare.

[1]S. Sun, C. B. Murray, D. Weller, L. Folks, and A. Moser, Science **287**, 1989 (2000).
[2]S. S. Kang, D. E. Nikles, and J. W. Harrell, J. Appl. Phys. **93**, 7178 (2003).
[3]T. Maeda, T. Kai, A. Kikitsu, T. Nagase, and J. Akiyama, J. Appl. Phys. **80**, 2147 (2002).
[4]O. Kitakami, Y. Shimada, K. Oikawa, H. Daimon, and K. Fukamichi, Appl. Phys. Lett. **78**, 1104 (2001).
[5]B. Jeyadevan, A. Hobo, K. Urakawa, C. N. Chinnasamy, K. Shinoda, and K. Tohji, J. Appl. Phys. **93**, 7574 (2003).
[6]B. Jeyadevan, K. Urakawa, A. Hobo, C. N. Chinnasamy, K. Shinoda, K. Tohji, D. D. Djayaprawira, M. Tsunoda, and M. Takahashi, Jpn. J. Appl. Phys., Part 1 **42**, L350 (2003).
[7]M. Chen and D. Nikles, J. Appl. Phys. **91**, 8477 (2002).
[8]J. Park and J. Cheon, J. Am. Chem. Soc. **123**, 5743 (2001).
[9]C. N. Chinnasamy, B. Jeyadevan, K. Shinoda, and K. Tohji, J. Appl. Phys. **93**, 7583 (2003).
[10]A. C. C. Yu, M. Mizuno, Y. Sasaki, M. Inoue, H. Kondo, I. Ohta, D. Djayaprawira, and M. Takahashi, Appl. Phys. Lett. **82**, 4352 (2003).
[11]Y. Sasaki, M. Mizuno, A. C. C. Yu, M. Inoue, K. Yazawa, I. Ohta, M. Takahashi, B. Jeyadevan, and K. Tohji, J. Magn. Magn. Mater. **282**, 122 (2004).
[12]Y. K. Takahashi, T. Koyama, M. Ohnuma, T. Ohkubo, and K. Hono, J. Appl. Phys. **95**, 2690 (2004).

JOURNAL OF APPLIED PHYSICS 97, 1 (2005)

Synthesis and magnetic properties of face-centered-cubic and hexagonal-close-packed Ni nanoparticles through polyol process

C. N. Chinnasamy[a] and B. Jeyadevan
Graduate School of Environmental Studies, Tohoku University, Sendai, 980-8579, Japan

A. Narayanasamy
Materials Science Center, Department of Nuclear Physics, University of Madras, Chennai, India

K. Shinoda and K. Tohji
Graduate School of Environmental Studies, Tohoku University, Sendai, 980-8579, Japan

K. Sato and S. Hisano
Dowa Mining Corporation, Saitama, Japan

(Presented on 11 November 2004)

The Ni nanoparticles with fcc or hcp phases have been synthesized in tetraethylene glycol by using the modified polyol process. The crystal structure has been controlled by changing the polyol/Ni mole ratio and the reaction temperature. The saturation magnetization of the as-prepared particles depends on the relative volume fraction of the hcp phase. The x-ray diffraction and extended x-ray absorption fine structure studies suggest the formation of pure fcc and hcp Ni phases. The hcp Ni particles show nonmagnetic behavior and thermally stable below 673 K. © *2005 American Institute of Physics*. [DOI: 10.1063/1.1851951]

I. INTRODUCTION

Nickel (Ni) is a ferromagnetic metal that crystallizes in fcc structure with a lattice parameter of 0.352 nm. Nickel films are widely used in electronics, chemical cells, battery, and in aerospace industry applications due to their ability to withstand corrosion and high temperatures. Though Ni is said to crystallize into fcc and hcp structures, hcp-Ni has never been found in nature and the synthesis of hcp-Ni received a great deal of attention in the past. However, there are only a few reports in the literature on the synthesis of hcp Ni using different techniques. The layers or powders of close packed hexagonal Ni have been electrolytically prepared nearly eight decades ago.[1,2] And also, nickel acetyl acetonate has been reacted with K/B alloy in an inert atmosphere to prepare hcp Ni powder.[3] In most of the methods, hcp-Ni was produced by inducing the formation through the use of substrate or by introducing defects.[4,5] Furthermore, there are contradicting theoretical reports[6] on the magnetic properties of hcp Ni. Here, we discuss the synthesis of Ni particles with two different crystal structures namely fcc and hcp by using modified polyol process along with their thermal stability and magnetic properties.

II. EXPERIMENT

The experiments were carried out using nickel acetate tetrahydrate [$(CH_3COO)_2Ni.4H_2O$, 99%, Wako] as a metal precursor. Specified amounts of metal precursors were introduced into 100 ml of either tetraethylene glycol (TEG) or trimethylene glycol (TMEG) and ultrasonicated for 5 min to dissolve the metal precursors. Then, the solution was transferred to a vessel with reflux attachment and placed in a mantle heater and heated to the boiling point of the solvent at a constant rate under gentle mechanical stirring. During this stage, metal precursor undergoes dissolution and is reduced to metal ions, and then the formation of nucleus and particle growth takes place. The Ni nanoparticles with fcc or hcp phases have been synthesized by varying the polyol/Ni mole ratio and the reaction temperatures.

The crystallographic phase of the particles was analyzed using x-ray powder diffraction (XRD) (Rigaku—Cu K_α radiation) technique. The morphology of the particles was examined by a direct observation via scanning electron microscopy (SEM) (Hitachi S-4100). The saturation magnetization (M_s) of the particles were measured at RT in a maximum applied field of 15 kOe using a vibrating sample magnetometer (Tamakawa model TM-VSM1230-HHHS) and wherever required with a superconducting quantum interference device magnetometer. The extended x-ray absorption fine structure (EXAFS) measurements at Ni–K absorption edge (8333 eV) were carried out by R-XAS Looper (RIGAGU Corporation) with fluorescence mode. Ti foil was kept before the sample in order to monitor incident x-ray intensity (I_0) by detecting the Ti–K fluorescence. The samples were put as a thin layer on a scotch tape. Fluorescent x-ray intensity (I_f) from the sample and Ti foil (I_0) was detected by scintillation counters.

III. RESULTS AND DISCUSSION

A. Structural characterization and magnetic properties

In polyol process, the metal particles are formed by the reduction of metal ions by polyol. Though the synthesis of metal particles with different crystal structures and particle diameters are possible using various types of polyol, we confine to TEG and TMEG only in this article. A series of ex-

[a]Electronic mail: chins@cir.tohoku.ac.jp

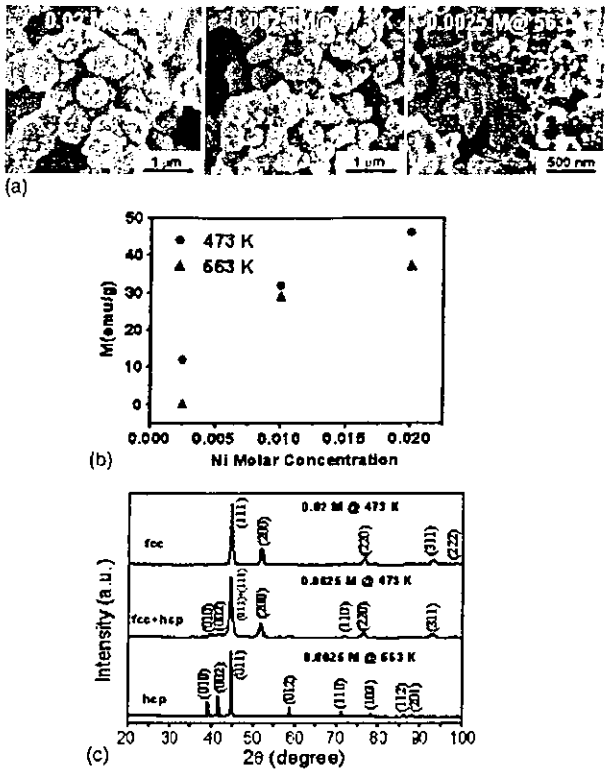

FIG. 1. (a) The SEM micrographs of Ni particles. (b) The relation between the Ni Metal ion concentration and magnetization of the Ni Particles synthesized in TEG at 473 and 563 K. (c) XRD patterns of the various phases of Ni particles.

periments were first carried out at 473 K in TEG for various nickel ion concentrations. The SEM micrographs of the samples synthesized with 0.02 and 0.0025 M nickel ion concentrations at 473 K are shown in Fig. 1(a). The presence of the agglomerated particles was observed for both the high and low concentrations and the size of the agglomerates decreased with decreasing metal ion concentration. The observed decrease in the size of the agglomerated particles is a consequence of low collision probabilities at lower nickel ion concentration. Besides, a decrease in the size of the particles that go to form these aggregates was also observed. The saturation magnetization (M_s) values of the Ni particles synthesized at 473 and 563 K for various Ni ion concentrations are shown in Fig. 1(b). The M_s decreased (compared with the bulk value of 55 emu/g) as the nickel ion concentration was reduced, indicating an increase in the relative volume of the nonmagnetic fraction from 0.17 at 0.02 M to 0.42 at 0.0025 M. The hysteresis loop of the fcc phase-dominant sample obtained from the reaction at 473 K for the 0.02 and 0.0025 M nickel ion concentrations are given in Fig. 2. The decrease of magnetization suggests that the nonmagnetic volume fraction increases with the decrease in the nickel ion concentration.

Figure 1(c) shows the XRD patterns of the samples synthesized with 0.02 and 0.0025 M of nickel ion concentrations in TEG at 473 K. When the crystal structure of these particles were analyzed, the particles synthesized with 0.0025 M of nickel, showed diffraction lines characteristics

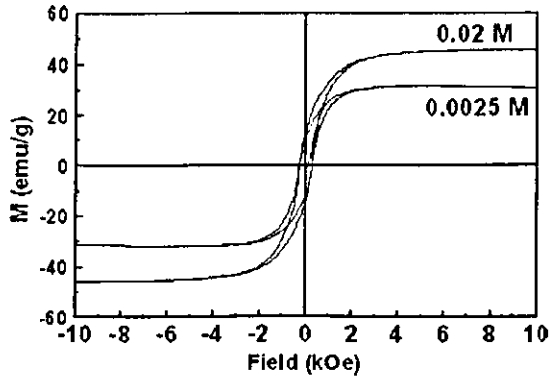

FIG. 2. The hysteresis loops the Ni particles synthesized in TEG with 0.02 and 0.0025 M nickel ion concentrations at 473 K.

to (010) and (002) lattice reflections of hcp-Ni. It should be noted that the main peak (011) of hcp-Ni coincides with that of the fcc Ni (111). Thus, the presence of (010) and (002) reflections is seen only when the relative volume fraction of the hcp phase is more than 0.45.

If the hcp phase can be induced by controlling the particle size, this can also be achieved either by using highly reducive polyol or reacting at higher temperatures. As TMEG is verified to be highly reducive, synthesis of Ni particles in TMEG at a nickel ion concentration of 0.0025 M at 473 K was carried out. The particles with diameters ranging between 60 and 80 nm were obtained. Furthermore, the magnetization of these particles was 32 emu/g, and suggests the presence of large amount of nonmagnetic fractions. Furthermore, the XRD showed the diffraction lines corresponding to hcp-Ni. However, pure nonmagnetic particles or disappearance of the reflections corresponding to fcc structure was not realized. Thus, the synthesis of particles at high temperature was attempted. As the boiling point of TMEG is about 483 K, the synthesis of Ni particles was carried out in TEG (boiling point ~593 K) at 563 K. The M_s of the Ni particles synthesized at 563 K with various nickel ion concentrations are presented in Fig. 1(b). In these experiments also the magnetization of the samples decreased as the nickel ion concentration was lowered. Furthermore, compared to the samples synthesized at 473 K, the M_s values were lower for all nickel ion concentrations experimented at 563 K. Especially for 0.0025 M, the particles are found to be nonmagnetic and this is a clear evidence for the nonexistence of fcc Ni phase. The SEM micrograph showed the particle size was approximately between 100 and 150 nm as shown in Fig. 1(a). As the synthesis temperature of hcp-Ni depended on the particle size, further reduction in particle diameter was attempted by introducing a nucleating agent, such as platinum.

The hcp-Ni particles with diameters ranging between 50 and 60 nm was synthesized by introducing small amount of Pt ions as seeds in TEG. Though the particles were fcc in structure at 433 K, it transforms to hcp-Ni completely at temperatures 563 K even for 0.01 M of nickel ion concentration.

Though, the appearance of reflections corresponding to hcp-Ni structure was recorded at the concentration as high as 0.01 M and temperatures as low as 473 K, the complete dis-

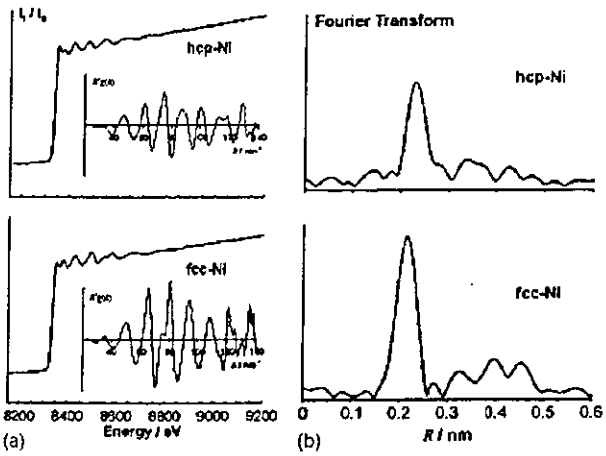

FIG. 3. (a) The x-ray absorption spectra measured as a function of I_f/I_0 ratio at Ni–K absorption edge for the hcp and fcc-Ni and k^3 weighted EXAFS spectra (inset figures) and the corresponding (b) Fourier transforms.

appearance of the diffraction lines corresponding to fcc structure was possible only for the Ni metal ion concentration of 0.0025 M at 563 K [Fig. 1(c)]. The particles synthesized under this condition were totally nonmagnetic. In a few cases, the nonmagnetic nature has been suggested the formation of Ni_3C. However, our XRD peak intensities did not match with Ni_3C and well fitted with hcp-Ni (JCPDS 45-1027) structure.[3] The formation of hcp-Ni phase was further confirmed by EXAFS analysis.

The I_f/I_0 ratio versus incident x-ray energy of the fcc and hcp-Ni particles are shown in Fig. 3. The difference between the two samples is recognized obviously in shape of oscillation. The difference is seen more clearly in the period of the EXAFS oscillation, which obtained by weighing of k^3 toward $\chi(k)$ extracted from the measured XAFS spectra. The fourier transform of $k^3\chi(k)$ spectra reflects the environmental atomic distribution around the absorbing atom of Ni. As shown in Fig. 3, interatomic distance of the first nearest neighbor shell in the hcp-Ni is farther than in fcc-Ni. In addition, width of the correlation peak is larger. These features suggest that the distance between nearest neighbor Ni–Ni pair correspond to 0.248 nm of fcc or 0.265 nm of hcp Ni and variation of the distance is due to the deviation from ideal hexagonal close packing in hcp-Ni. The FEFF (an *ab initio* theoretical code) calculations[7] may provide further information about the local structure of hcp Ni.

B. Thermal stability

Though the hcp-Ni phase was stable at 563 K in polyol, their temperature stability was determined by *ex situ* annealing under an inert atmosphere. The pure nonmagnetic hcp nickel sample was annealed at 673 and 773 K. Though the transformation of the bulk hcp to fcc phase has been

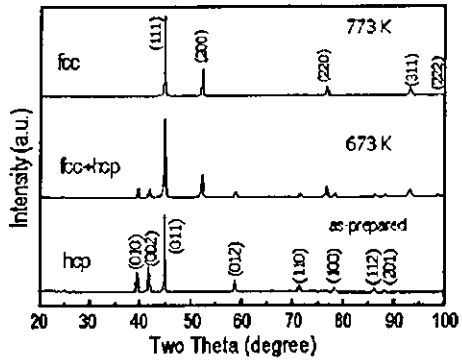

FIG. 4. The XRD patterns of the hcp Ni nanoparticles synthesized with 0.0025 M nickel ion concentration in TEG at 563 K were externally annealed at different temperatures.

reported[3] to be around 673 K, the magnetization of the present sample annealed at 673 K for an hour is only 15.5 emu/g. This suggests that only less than 30% of the particles are converted to the fcc phase. On the other hand, the magnetization of the sample annealed at 773 K is 52 emu/g, which indicates that the hcp particles are unstable at this temperature. The intense diffraction lines corresponding to the hcp phase (010), (002) disappeared in the sample annealed at 773 K as shown in Fig. 4.

IV. CONCLUSION

In conclusion, a comparatively easy and reliable method to synthesize fcc and hcp-Ni nanoparticles has been proposed. The primary particle size has been found to play a decisive role on the crystal structure of the particles. However, the reaction temperature is also found to influence the critical grain size for the hcp-Ni. The hcp-Ni nanoparticles show nonmagnetic behavior and thermally stable below 673 K.

ACKNOWLEDGMENTS

This study was supported by Grant-in-Aid for Basic Research Nos. (B)15360003, (S)14103016, and (S)13852016 from the Ministry of Education, Science, Culture and Sport of Japan and No. H14-nano-021 from the Ministry of Health, Labor and Welfare.

[1]G. Bredig and R. Allolio, Z. Phys. Chem., Stoechiom. Verwandtschaftsl. 126, 41 (1927).
[2]G. P. Thomson, Nature (London) 123, 912 (1929).
[3]G. Carturan, G. Cocco, S. Enzo, R. Ganzerla, and M. Lenarda, Mater. Lett. 7, 47 (1988).
[4]M. K. Datta, S. K. Pabi, and B. S. Murty, J. Mater. Res. 15, 1429 (2000).
[5]Vergara and V. Madurga, J. Mater. Res. 17, 2099 (2002).
[6]D. A. Papaconstantopoulos, J. L. Fry, and N. E. Brener, Phys. Rev. B 39, 2526 (1989).
[7]J. J. Rehr and A. L. Ankudinov, J. Synchrotron Radiat. 8, 61 (2001).

Available online at www.sciencedirect.com
SCIENCE DIRECT®
ELSEVIER
Journal of Magnetism and Magnetic Materials ▮ (▮▮▮▮) ▮▮▮–▮▮▮
Journal of magnetism and magnetic materials
www.elsevier.com/locate/jmmm

Preparation and properties of ferromagnetic FePt dispersion

K. Sato[a], B. Jeyadevan[b,*], K. Tohji[b]

[a]*Dowa mining company, Daiichi Takko building. 1-8-2, Marunouchi Chiyada ku, Tokyo 100-8282, Japan*
[b]*Graduate School of Environmental Studies, Tohoku University, Aoba 20, Aramaki Aza Aoba ku, Sendai 980-8579, Japan*

Abstract

FePt nanoparticles were prepared via the coreduction of platinum and iron acetyl acetonate precursors in tetraethylene glycol at various temperatures. The X-ray diffractogram of the as-synthesized FePt nanoparticles at temperatures above 573 K exhibited (0 0 1) and (1 1 0) superlattice reflections. TEM–EDX studies revealed that the average particle diameter was 5 nm with nearly equiatomic composition. The saturation magnetization and coercivity at room temperature (RT) were found to be 50 emu/g and 2.1 kOe, respectively. The high anisotropy field of about 32 kOe and magnetic ordering at RT revealed the presence of the highly anisotropic $L1_0$ phase. These particles were partially dispersed in an organic solvent using oleyl amine as surfactant. The dispersed FePt nanoparticles will be useful in future technological applications.

PACS: 61.46.+*w*; 75.50T$_i$; 75.50.Bb; 75.50.Ss

Keywords: FePt nanoparticles; FePt; Dispersed FePt; FePt magnetic fluids; High coercivity

1. Introduction

Ferrofluids have received much attention in the past due to their interesting properties, which can be used to develop new technologies such as spin valves, hyperthermia, novel inks for inkjet printers and high density recording media [1–4]. Many possible applications of ferrofluids necessitate two material prerequisites—high remanent magnetization (M_r) and high anisotropy (K_u) at room temperature (RT) (of the order of 10^6–10^7 erg/cm^3). While the high M_r is a characteristic nature of soft ferromagnetic materials, the high K_u is a feature of hard magnetic materials like FePt and CoPt. Hence, the preparation of bimetallic ferrofluids with higher magnetization and coercivity at RT is a challenging one. However, most of the chemical synthesis techniques reported so far require an indispensable post-annealing step to obtain the highly anisotropic $L1_0$ phase of FePt or CoPt nanoparticles, which seriously affects the bimetallic ferrofluids preparation and impedes the development of high-density magnetic recording media. The FePt particles synthesized via chemical route are reported to be superparamagnetic with a chemically disordered FCC structure [4]. The authors have already reported that the ordering temperature and the magnetic properties of the as-prepared FePt and CoPt nanoparticles synthesized through the modified polyol process were sensitive to the reaction conditions [5–7]. The formation of the FCC phase or the partially ordered $L1_0$-FCT phase and their particle size depend on the reaction kinetics, which is controlled by the type of polyol, reaction temperature and Fe/Pt mole ratio. The simultaneous reduction is also dependent on the

*Corresponding author. Tel.: +81 022 217 7391; fax: +81 022 217 7391.
E-mail address: jeya@mail.kankyo.tohoku.ac.jp (B. Jeyadevan).

0304-8853/$ - see front matter © 2004 Elsevier B.V. All rights reserved.
doi:10.1016/j.jmmm.2004.11.002

difference in redox potential of metal compounds. Though the ordered FCT structure is the stable phase, often-encountered disordered FCC structure of the as-synthesized particles is thought to be a consequence of the fast reaction kinetics. Therefore, this has limited the direct synthesis of $L1_0$ FePt particles by using chemical methods. Here, we report the direct synthesis of the partially ordered FCT–FePt nanoparticles ferrofluids using the modified polyol process and also its structure, morphology and magnetic properties. The as-prepared ferrofluids are highly stable against oxidation.

2. Experimental

Specified amounts of Fe and Pt acetylacetonate precursors were dissolved in 100 ml of tetraethylene glycol (TEG) in a reaction vessel with a reflux attachment and placed in a mantle heater and heated at a constant rate under gentle mechanical stirring, and the suspension was refluxed for $3\frac{1}{2}$ h at specific temperatures between 533 and 593 K at 10 K interval. During this stage, generally, the pale yellow colored solution turned colorless and finally black suggesting the formation of FePt particles. Olelamine and Oleic acid were introduced to the suspension and then particles were transferred to the hexane medium through liquid–liquid extraction.

The structure, morphology, composition and magnetic properties of the as-prepared FePt particles were analyzed using X-ray diffraction (XRD) (Rigaku–Cu-K_α radiation), high-resolution transmission electron microscopy (HRTEM- Hitachi HF2000), energy dispersive X-ray spectroscopy (EDX) in TEM and vibrating sample magnetometer, respectively. The anisotropy field (H_k) was measured by using a torque magnetometer at RT with a maximum applied field of 25 kOe.

3. Results and discussion

The XRD analysis in Fig. 1 showed that the FePt nanoparticles synthesized at 473 K (sample A) were FCC in structure, whereas the samples synthesized at 573 K (sample B) showed (0 0 1) and (1 1 0) superlattice lines, indicating a significant degree of $L1_0$ ordering in the as-prepared state.

The TEM micrograph of the pre-dispersed agglomerated particles of sample B is shown in Fig. 2. Though the TEM micrograph showed particles with diameter between 5 and 10 nm, XRD analysis gives an average grain size of about 4 nm.

The FePt nanoparticles of samples A and B were ferromagnetic at RT. The magnetization (M_s) and coercivity (H_c) of sample A were 15.6 emu/g and 32 Oe, respectively.

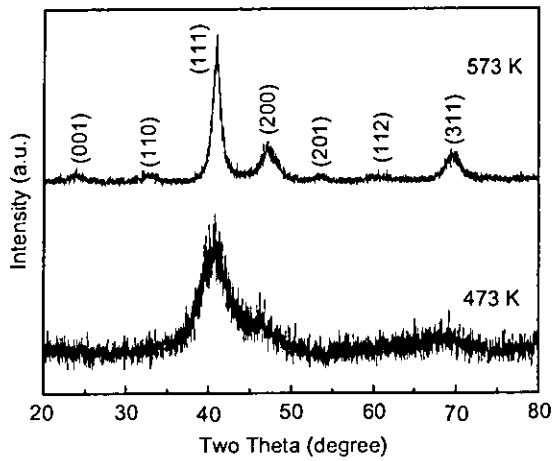

Fig. 1. X-ray diffraction patterns of the FePt nanoparticles synthesized at 473 and 573 K in TEG.

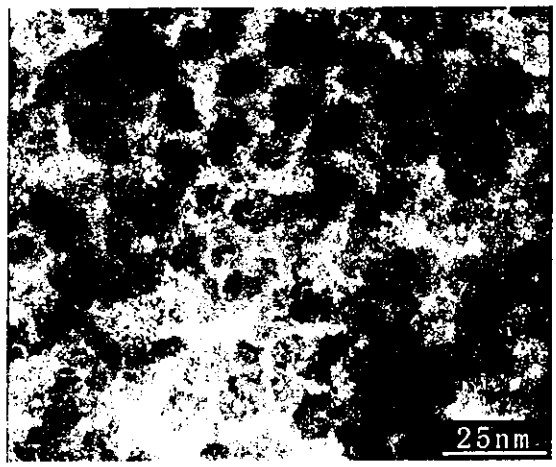

Fig. 2. TEM micrograph of the as prepared, pre-dispersed partially ordered FCT–FePt nanoparticles.

In contrast, sample B showed the RT magnetic properties as given in Fig. 3. The magnetization and coercivity were 50 emu/g and 2.1 kOe, respectively, whereas the particles of Sun et al. [4] exhibited superparamagnetism in the as-prepared state and required annealing at least at 833 K for 30 min under 1 atm of N_2 gas to become ferromagnetic. The enhancement in the coercivity of the present sample compared to 370 Oe reported in our earlier report [7] was due to the modification in the synthesis procedure, for example, by controlling the reaction rate, particle size distribution, etc. The moderate value of 2.1 kOe for the coercivity of sample B could be attributed to the magneto-static interaction as confirmed by the negative value obtained from δM studies [7].

To confirm the formation of the highly anisotropic FCT phase, the intrinsic magnitude of the magnetic

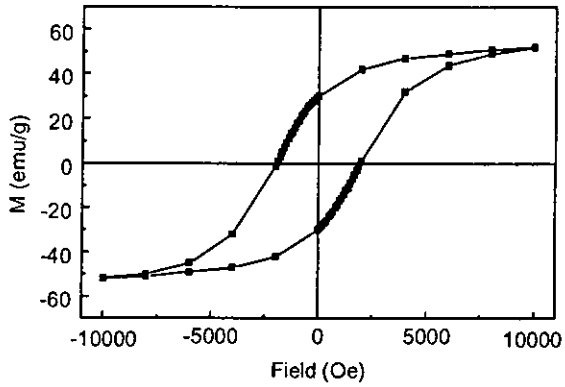

Fig. 3. RT hysteresis loop for FePt nanoparticles synthesized at 573 K.

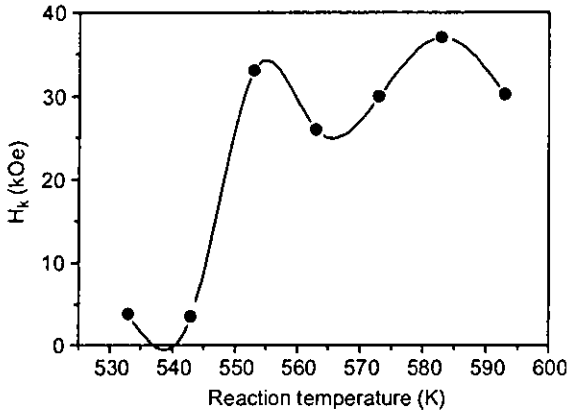

Fig. 4. H_k vs. reaction temperature of FePt nanoparticles (line is a guide to the eye).

anisotropy field "H_k" of the particles was measured by carrying out the rotational hysteresis loss analysis. The magnetic field obtained by extrapolating the linear part of W_r curve at high fields to $W_r = 0$, is the intrinsic anisotropy field (H_k). W_r is defined as

$$W_r = \int_0^{2\pi} L \, d\theta,$$

where L is the hysteresis loss and θ is the angle of rotation. The H_k versus temperature plot given in Fig. 4 shows that the $L1_0$ phase is formed under reaction temperatures above 553 K. The H_k of the as-synthesized sample at 573 K was 32 kOe.

Thus, it could be concluded that the reaction temperature of 573 K is high enough to obtain FePt particles with a considerable degree of ordering.

However, to determine the magnetic properties of individual nanoparticles, the as-prepared FCT–FePt particles have to be dispersed in a solvent. Thus, the as-prepared partially ordered FePt particles were dispersed in an organic solvent using oleylamine and oleic acid as surfactants. The appropriate amounts of surfactants were introduced into the FePt–polyol suspension. Then, the suspension is agitated for 10 h using a mechanical shaker. Then, a non-polar solvent such as hexane is added to the suspension and agitated further. During this process, the particles that get coated with the surfactants are transferred from the polyol to the hexane medium. The solid concentration in the hexane medium can be controlled by precipitation using bad solvent and redispersion in hexane or in any other non-polar solvents. The TEM micrograph of the dispersed particles and their particle size distribution is shown in Fig. 5(a) and (b), respectively. The average diameter of the particles that came into dispersion was 5 ± 1 nm and the polycrystalline nature of the particle was confirmed. Any difference between TEM and XRD crystallite size can be due to polycrystallinity of the

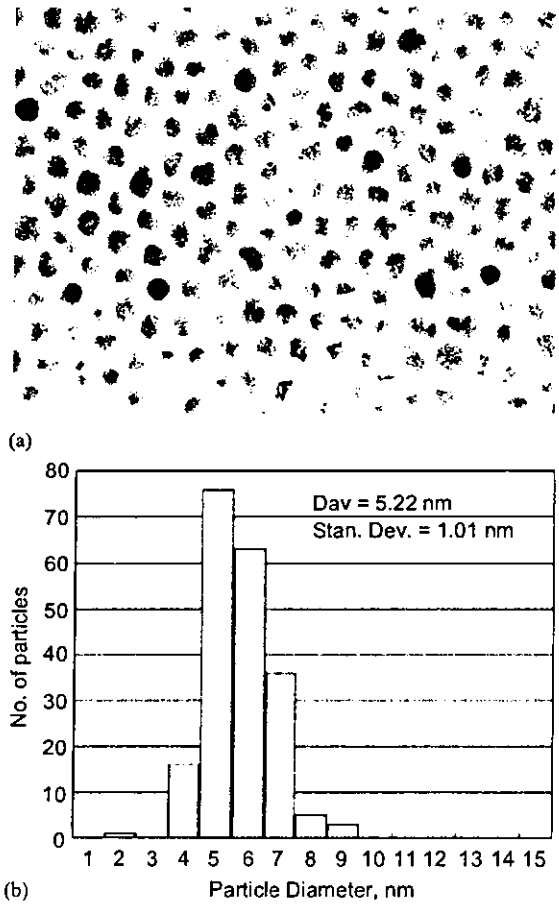

Fig. 5. (a) TEM micrograph of individually dispersed FCT–FePt nanoparticles and (b) particle size distribution.

particles. Though the particles are brought to dispersion, the dispersed particles seem to show platinum-rich ($Fe_{30}Pt_{70}$) composition compared to the powder ($Fe_{50}Pt_{50}$). Consequently, the magnetic properties of

the dispersion become inferior to that of the powder. The main reason for this is the composition dependent magnetic properties rather than the dipolar interactions between particles. The reason for selective dispersion of platinum-rich particles is not yet clear and is being investigated.

In conclusion, ferromagnetic FePt nanoparticles with diameter of about 5–10 nm, and magnetization and coercivity of 50 emu/g and 2.1 kOe were obtained by modified polyol process by using TEG. The presence of the $L1_0$ FePt phase was confirmed by XRD and rotational hysteresis measurement. The FePt particles dispersion was achieved by using surfactants such as oleylamine and oleic acid. The compositional difference in particles between the powder and the dispersion is being studied.

Acknowledgment

This study was supported by Grant-in-Aid for Basic Research #(B) 15360003, #(S) 14103016, and #(S) 13852016 from the Ministry of Education, Science, Culture and Sport of Japan and # H14-nano-021 from the Ministry of Health, Labor and Welfare.

References

[1] J.C. Lodder, D.J. Monsma, R. Vlutters, T. Shimatsu, J. Magn. Magn. Mater. 198–199 (1999) 119.
[2] A. Jordan, R. Scholz, P. Wust, H. Schirra, T. Schiestel, H. Schmidt, R. Felix, J. Magn. Magn. Mater. 194 (1999) 185.
[3] C. Kormann, E. Schwab, F.W. Raulfs, K.H. Bech, US Patent 5 500 (1996) 141.
[4] S. Sun, C.B. Murray, D. Weller, L. Folks, A. Moser, Science 287 (2000) 1989.
[5] B. Jeyadevan, A. Hobo, K. Urakawa, C.N. Chinnasamy, K. Shinoda, K. Tohji, J. Appl. Phys. 93 (2003) 7574.
[6] C.N. Chinnasamy, B. Jeyadevan, K. Shinoda, K. Tohji, J. Appl. Phys. 93 (2003) 7583.
[7] B. Jeyadevan, K. Urakawa, A. Hobo, C.N. Chinnasamy, K. Shinoda, K. Tohji, D.D. Djayaprawira, M. Tsunoda, M. Takahashi, Jpn. J. Appl. Phys. 42 (2003) L350.

ナノ粒子における格子歪と磁気特性

Structural Distortions in Nanometer Particles and Their Magnetic Properties

羽田紘一　石巻専修大学理工学部
K. Haneda, Faculty of Science and Engineering, Ishinomaki Senshu University

The magnetism of fine particles involves both size and surface effects due to their large specific surface area. Evidence has been accumulating that fine particles possess properties that can differ substantially from those of bulk materials. Structural peculiarities associated with distorted structure on the surface and in the bulk, and peculiarities in the intrinsic magnetization of these small particles, are the main subjects reviewed in this paper. Magnetic hardening arising from stress-induced anisotropy and surface anisotropy in some ferrite particles is also discussed.

Key words: magnetic small particles, surface magnetism, surface anisotropy, magnetic hardening, core-shell model, non-collinear structure, ferrite, lattice distortion

1. はじめに

磁性微粒子はこれまで，永久磁石，情報の記録媒体，および磁性流体と工業的にも重要な位置を占めてきた[1),2)]．また最近では微粒子薄膜として新たな応用を目指す試みや[3)]，高密度情報記録を意図した量子化磁気ディスクとして，ナノドット（量子ドット）配列構造の磁気的挙動が注目されている[4)]．ナノ構造化に伴う機能性への影響を明らかにし制御につなげることは，この分野の材料設計の観点からも望まれる．最近の動向として，磁性微粒子の新たな応用探査として，バイオ応用への試みが各方面で進展しつつあるようである．筆者らも微粒子と生体親和性の観点から，サイズ効果および表面効果の両面から細胞機能試験と動物実験での評価を厚生労働科研費（課題番号 H14-ナノ-021）の支援を受けて進めている．

微粒子と一言でいっても，金属系微粒子と酸化物系微粒子とではその背後に控える事情はかなり異なる．第一に，当該物質として認識される最小サイズすなわち単位胞 (unit cell) のサイズに大きな違いがある．1 立方ナノ粒子を考えた場合，Fe, Ni, Co 系の金属・合金系であれば数個以上の単位胞があることになる．例えば bcc Fe は，0.29 nm の格子定数より単位胞は 0.024 nm^3 の大きさであり，1 立方ナノ粒子は約 40 個の単位胞に相当する．Fe_3O_4 のようなスピネル型フェライトでは格子定数は 0.8 nm，YIG などのガーネット型フェライトでは 1.2 nm，六方晶系フェライトでは単位胞のサイズはさらに大きくなり，1 個の単位胞にも相当しなくなる．また金属強磁性体とイオン性（絶縁性）強磁性体では，強磁性を導く主役が金属では自由電子（巡回電子）であるのに対しイオン性物質では束縛電子（局在電子）であり，磁性原子間の相互作用も前者では近接相互作用である交換相互作用に対し，後者は遠距離相互作用である超交換相互作用が主体として働く．したがってサイズ効果が顕在化するサイズ領域やサイズ効果そのものが異なっているであろうことは容易に想像がつく．

微粒子における特異磁性は，よく知られているようにサイズ効果として磁区構造の変化に起因の技術的磁化に現れるばかりでなく，微粒子という幾何学的構造上の制約を受け物質固有の結晶構造や磁気的性質にも現れる[1),2),5),6)]．また技術的磁化における magnetic hardening のメカニズムにおいても，通常の結晶磁気異方性や形状磁気異方性に加えて，表面磁気異方性や歪磁気異方性が付与された形で微粒子の磁気的挙動に変調を与えることとなる．以下に具体的な実験データを提示しつつ概説することとする．筆者がこの分野の研究を遂行するにあたり，メスバウアー分光を主要な分析手段として進めてきたこともあり，本稿でもそのバイアスがかかっていることをご了解いただきたい．特にナノ粒子の構造に起因する格子歪の観点から，ナノ粒子の特異磁性の起因に迫ることとする．

2. ナノ粒子の磁性とそれを律する要因

ナノ粒子の磁性がバルクの磁性と異なる由縁は，サイズが小さいことによるサイズ効果からの寄与がある点，および結合配位数がバルク内原子より減少の表面原子を多量に含む粒子表面層の占める割合が大きいことによる表面効果からの寄与があるの 2 点である．

磁化過程・減磁過程における磁気特性の違い（技術磁化）は，古くから確立されているように大方サイズ効果に起因するものである．後述のように，微粒子化に伴う磁区構造の変化がその背景にある．

一方，物質定数と考えられてきた物理量，例えば自発磁

化値（すなわち飽和磁化値でいわゆる固有磁化）は，ナノ化によって大きく変わること（通常は低下）が，多くの報告で指摘されており，筆者らのこれまでの研究でそれは粒子表面層あるいは表面構造において，バルク体とは異なるnon-collinearの特異な磁気構造（spin canting構造と命名）が存在することがその原因（表面効果）として確立しつつある[1),2),7)~10)]．この特異な磁気構造は，フェライト系微粒子のようなイオン性（絶縁性）強磁性体では多くの物質で一般的に観測されている現象で，core-shellモデルが普遍的に成立するということで大方の磁性は説明がつく．しかし金属強磁性体では局所的な磁化の増大が見られることはあるものの[5)]，この特異な磁気構造はまだ観測されていない．強磁性を導く主役の電子が一方では局在電子であるのに対し，他方では巡回電子であることの反映と見ることもできる．

これとは逆に，磁気（自発磁化）をもたないとされる物質でもナノ化によって巨大磁化値が観測される事例や，ネール点などの磁気転移温度に粒子サイズ依存性が観測される事例もあり，その原因の究明が待たれる．ナノ粒子の構造と物性を律する要因として，粒子表面層を占める原子数が多いことに端を発するバルク体とは異なる結晶構造（微粒子全域あるいは表面域）の誘発や，イオン性物質ではバルク体とは異なるイオン配置[11)]や空格子の出現，温度によるイオンの再配列など，エネルギー的に有利なさまざまな形で特異構造を誘発しバルク体とは異なる固有の物性を呈することとなる．これらについては本稿の中心的課題として，具体例を提示して詳述するとして，まずは磁性微粒子のごく一般的な性質として，微粒子化に伴う磁区構造の変化について触れておく．

3. 磁区構造の変化と超常磁性現象

よく知られているように，強磁性物質は磁区構造と呼ばれる構造をとっている．すなわち，各結晶粒内は磁区と呼ばれるいくつかの小領域に分かれており，この小領域内にある自発磁化は飽和まで磁化されているが，領域ごとそれぞれ磁化の方向が異なるいわゆる多磁区構造である．磁気に関与のエネルギーの総和（交換・異方性・磁歪・静磁エネルギーなど）が関係し，とりわけ磁区間の静磁エネルギーが最小となるような配置をとっているのである．しかし強磁性体粒子はその粒子径を減少させると，粒子内に磁区の境界（磁壁）が存在しないほうがエネルギー的により安定となり一つの粒子が一つの磁区からなる，いわゆる単磁区粒子となる．単磁区粒子内では磁気秩序状態が保たれており磁化の向きは一様で，磁気異方性エネルギーを最小にするような特定の方向に向いている場合が安定である．磁気異方性には結晶構造に起因する結晶磁気異方性，磁性微粒子の形状や歪に起因する形状磁気異方性，歪磁気異方性，それと本稿で以下に取り上げる表面磁気異方性も含まれる．

多磁区構造を有する結晶粒集合体の磁化過程および減磁過程は大方エネルギー的に少なくてすむ磁壁の移動によって起こるために，磁気履歴曲線の横幅は狭く保磁力H_cも小さい．しかし単磁区粒子の集合体では異方性エネルギーに抗しての磁化の回転によってそれが起こるために磁気履歴曲線の幅は大きく，大きな保磁力H_cが得られる．一方，粒子径が極端に小さくなると，粒子内の磁化の方向が熱的動揺を受けて不安定になってくる．すなわち粒子のもつ異方性エネルギーKV（Kは異方性定数，Vは粒子の体積）に比較して，熱振動のエネルギーkT（kはボルツマン定数，Tは温度）が大きくなるのでもはや磁化の方向は一定の安定な方向はとれなくなり，粒子1個があたかも大きい磁気能率をもった常磁性イオンのように振舞う，いわゆる常磁性を示すようになる．このような粒子は磁気履歴曲線を示さず，これが混在することにより保磁力H_cが減少する．超常磁性を示す微粒子では磁化曲線$M(H, T)$はヒステリシスを示さずH/Tで描くと超常磁性の理論から期待されるLangevin関数$M/M_s=\coth(mH/kT)-(kT/mH)$で表せる一定の曲線状にのるようになる．ただしここでHは磁場，M_sは飽和磁化，mは粒子1個の磁気モーメントを表す．

4. 微粒子における格子歪の起因

微粒子は気相・液相・固相反応や高速ボールミルを用いた粉砕などにより生成される．多くは熱力学的非平衡状態下もしくはそれに近い条件下で，結晶粒成長を抑えての生成である．そこには構造相転移が介在することもあるし，相変態に伴う格子歪が粒子形態に影響を及ぼすこともありうる．イオン性物質であれば，格子歪に伴う異常なイオン配置や空格子の生成を誘導する要因ともなる．また同一物質であっても生成プロセスによって導入される格子歪の様相に差異が生ずる場合もありうる．

粒子サイズの縮小につれて表面原子層の占める割合は当然多くなる．表面原子は結合に与る配位数の観点からは，バルク内の原子に比して減少の状態にあり，粒子形成に際しては余分な表面エネルギーがかかわることとなる．その影響は粒子全域に及ぶこともあれば表面域に留まることもある．また構造的には後述の表面磁気異方性や歪磁気異方性を誘発し磁気的な硬質化をもたらすこともある．

具体例としてFe, Coなどの金属系微粒子では，粒子サイズにより表面エネルギーとバルク体の自由エネルギーのバランスが変わり微粒子状態の結晶相に異変が起こることがある．バルク体のFeは室温ではbccであるが，高温域(1183~1663 K)ではfccである．またバルク体のCoは室温ではhcpであるが，高温域(>695 K)ではfccである．Kitakamiらは，高めの不活性ガス圧下でのスパッタ法で生成した30 nm以下のCo微粒子は室温でfcc構造をと